[redacted]

MARTIN MARIETTA ENERGY SYSTEMS LIBRARIES
3 4456 0360821 9

ORNL 827
Progress Report

8A
CENTRAL RESEARCH LIBRARY
DOCUMENT COLLECTION

AEC RESEARCH AND DEVELOPMENT REPORT

Inv. 60

[redacted]

DECLASSIFIED
By Authority
LABORATORY RECORDS
1954

METALLURGY DIVISION

QUARTERLY PROGRESS REPORT FOR PERIOD ENDING JULY 31, 1950

CENTRAL RESEARCH LIBRARY
DOCUMENT COLLECTION
LIBRARY LOAN COPY
DO NOT TRANSFER TO ANOTHER PERSON
If you wish someone else to see this document, send in name with document and the library will arrange a loan.

DECLASSIFIED
Classification Changed To:
By Authority
By:

OAK RIDGE NATIONAL LABORATORY
OPERATED BY
CARBIDE AND CARBON CHEMICALS DIVISION
UNION CARBIDE AND CARBON CORPORATION
UCC
POST OFFICE BOX P
OAK RIDGE, TENNESSEE

[redacted]

[redacted]

ORNL-827

This document consists of 82 pages. Copy 8 of 103 Series A.

Contract No. W-7405, eng 26

METALLURGY DIVISION

J. H. Frye, Jr., Director

QUARTERLY PROGRESS REPORT

for Period Ending July 31, 1950

Edited by

E. C. Miller and W. H. Bridges

DATE ISSUED DEC 4 1950

OAK RIDGE NATIONAL LABORATORY
operated by
CARBIDE AND CARBON CHEMICALS DIVISION
Union Carbide and Carbon Corporation
Post Office Box P
Oak Ridge, Tennessee

[redacted]

[redacted]

MARTIN MARIETTA ENERGY SYSTEMS LIBRARIES

3 4456 0360821 9

[redacted]

1 G. T. Felbeck (C&CCD)
2-3 706-A Library
4 706-B Library
5 Biology Library
6 Health Physics Library
7-8 Training School Library
9 Metallurgy Library
10-13 Central Files
14 C. E. Center
15 C. E. Larson
16 W. B. Humes (K-25)
17 W. D. Lavers (Y-12)
18 A. M. Weinberg
19 J. A. Swartout
20 E. J. Murphy
21 F. C. VonderLage
22 J. H. Frye, Jr.
23 E. H. Taylor
24 A. H. Snell
25 A. Hollaender
26 F. L. Steahly
27 K. Z. Morgan
28 D. W. Cardwell
29 M. T. Kelley
30 W. H. Pennington
31 E. C. Miller
32 W. H. Bridges
33 A. G. H. Anderson
34 L. K. Jetter
35 E. J. Boyle
36 W. D. Manly
37 E. D. Shipley
38 R. S. Livingston
39 C. P. Keim
40 G. H. Clewett
41 C. D. Susano
42 W. W. Parkinson
43 R. J. Gray
44 B. S. Borie
45 D. S. Billington
46 C. D. Smith
47 D. E. Hamby
48 E. E. Stansbury
49 G. P. Smith
50 J. E. Cunningham
51-52 Central Files (O.P.)

External Distribution

53-60 Argonne National Laboratory
61-63 Atomic Energy Commission, Washington
64-67 Brookhaven National Laboratory
68-69 Knolls Atomic Power Laboratory
70-71 General Electric Company, Richland
72 Hanford Directed Operations (All Technical Quarterlies)
73-76 Los Alamos
77-78 New York Operations Office
79 Patent Branch, Washington
80-94 Technical Information Branch, ORE
95-98 University of California Radiation Laboratory
99 Massachusetts Institute of Technology (Kaufmann)
100 Battelle Memorial University
101-103 NEPA

[redacted]

[redacted]

TABLE OF CONTENTS

SUMMARY 7

REACTOR FUEL PROBLEMS 10
- Bonding and Diffusion in ORNL (Clinton) Slugs 10
- Gases in Blisters in MTR Fuel Elements 10
- Thermal Cycling of Hanford Slugs 11
- Extrusion and Drawing of Uranium 13

THORIUM PROGRAM 16
- Thorium Alloy Development 16
- Yield Point of Thorium 16
- Impact Testing of Thorium 28

REACTOR COMPONENT ASSEMBLY FABRICATION 30
- Materials Testing Reactor Fuel Assemblies 30
- Bulk Shielding Facility Fuel Assemblies 30
- Bonding Uranium to Other Metals 31
- Lead Creep for MTR Neutron Window 34

PREFERRED ORIENTATION AND ANISOTROPY IN PROPERTIES OF METALS 35

MECHANICAL PROPERTIES OF METALS 50
- Uranium Creep Testing 50
- Heat and Liquid Metal Resistant Alloy Testing 50
- Pure Metals--Deformation Research 50

AIRCRAFT NUCLEAR PROPULSION--MATERIALS PROGRAM 52
- Static Corrosion Testing 52
- Circulating Corrosion Testing 70
- ANP Fuel Element Fabrication Program 71

FUNDAMENTAL RADIATION EFFECTS INVESTIGATION 72
- Effect of Neutron Irradiation on Copper Alloys 72
- In-pile Creep Experiment 77

SERVICE WORK 78
- Melting, Drawing and Extrusion 78
- Rolling Mill 78

PERSONNEL 81

[redacted]

[redacted]

LIST OF FIGURES

Fig. 1	Gamma Extrusion of Natural Uranium	14
Fig. 2	Natural Uranium Bars	15
Fig. 3	Load-Elongation Curve for Westinghouse Thorium	18
Fig. 4	Compression Load-Strain Curve for Ames Thorium	20
Fig. 5	Compression Test Specimen of Ames Thorium	21
Fig. 6	Load-Elongation Curve of Annealed Ames Thorium	23
Fig. 7	Load-Elongation Curve of Cold-Rolled Ames Thorium	24
Fig. 8	Thorium Tensile Specimens, Annealed	26
Fig. 9	Photograph of Thorium Tensile Specimen, Cold-Rolled	27
Fig. 10	Thorium Impact Test (Ames) Charpy	29
Fig. 11	Silver to Silver Bond with Mercury	33
Fig. 12	Silver Bonded to Silver Bonds with Tin	33
Fig. 13	Photomicrographs Showing the Deformed Grain Structure of the Sample of α-Extruded Uranium from Which the X-ray Diffraction Specimens Were Machined	36
Fig. 14	Sketch Showing the Dimensions of the X-ray Diffraction Specimens and the Locations in the Sample of α-Extruded Uranium from Which They Were Machined	37
Fig. 15	Preferred Orientation Plot - (110) - α-Extruded Uranium	38
Fig. 16	Preferred Orientation Plot - (021) - α-Extruded Uranium	39
Fig. 17	Preferred Orientation Plot - (002) - α-Extruded Uranium	40
Fig. 18	Preferred Orientation Plot - (111) - α-Extruded Uranium	41
Fig. 19	Preferred Orientation Plot - (112) - α-Extruded Uranium	42
Fig. 20	Preferred Orientation Plot - (131) - α-Extruded Uranium	43
Fig. 21	Preferred Orientation Plot - (040) - α-Extruded Uranium	44
Fig. 22	Preferred Orientation Plot - (023) - α-Extruded Uranium	45
Fig. 23	Preferred Orientation Plot - (200) - α-Extruded Uranium	46
Fig. 24	Preferred Orientation Plot - (113) - α-Extruded Uranium	47
Fig. 25	Type 310 Stainless Steel Exposed to Molten Lithium, 1000°C for 40 hrs	56

[redacted]

Fig. 26 Type 316 Stainless Steel Exposed to Molten Lithium, 1000°C for 40 hrs 57

Fig. 27 Type 304 Stainless Steel Exposed to Molten Lithium, 1000°C for 40 hrs 58

Fig. 28 Type 347 Stainless Steel Exposed to Molten Lithium, 1000°C for 40 hrs 59

Fig. 29 Type 405 Stainless Steel Exposed to Molten Lithium, 1000°C for 40 hrs 60

Fig. 30 Type 446 Stainless Steel Exposed to Molten Lithium, 1000°C for 40 hrs 61

Fig. 31 Type 430 Stainless Steel Exposed to Molten Lithium, 1000°C for 40 hrs 62

Fig. 32 Sectional View Vacuum Argon Corrosion Testing Apparatus 67

Fig. 33 Corrosion-Liquid Pb-U and Bi-U Alloys 68

Fig. 34 Corrosion-Liquid Pb-U and Bi-U Alloys 69

Fig. 35 Change of Electrical Resistance During Irradiation of Copper Containing 2% Be(wt) 73

Fig. 36 Isothermal Annealing Curves for Copper Containing 9.5% Al (at) 75

[redacted]

LIST OF TABLES

Table I	Thermal Cycling of Uranium Bars	12
Table II	Westinghouse Thorium—Conventional Tensile Test Data	19
Table III	Vickers and Rockwell Hardness—Ames Compression Test Bars	22
Table IV	Ames Thorium—Conventional Tensile Test Data	25
Table V	Impact Strength of Thorium	28
Table VI	Corrosion Results of Stainless Steels in 1000°C Lithium	53
Table VII	Corrosion Data on the Pure Metals in 1000°C Lithium	64

[redacted]

[redacted]

SUMMARY

ORNL Slug Problem. The investigation of diffusion between the uranium slug and its aluminum jacket as a possible contributing factor in the failure of ORNL reactor slugs in service has been largely completed. The use of an aluminum-silicon brazing alloy bond between slug and container has been recommended to lessen failure resulting from diffusion, and limited operating tests on Al-Si bonded slugs substantiate the recommendation.

Blisters in MTR Fuel Elements. The gas in blisters in MTR fuel plates has been analyzed and found to be predominantly hydrogen, tending to confirm the belief that the blistering results from absorption of water in plate surfaces prior to cladding, which reacts with the material during annealing after cladding.

Thermal Cycling of Hanford Slugs. This program has indicated that thermal cycling produced with the thermal gradient equipment will not duplicate the distortion which occurs in the Hanford reactors; the experimental work is therefore being concluded.

Extrusion and Drawing of Uranium. A study is in progress to determine the feasibility of producing natural uranium slugs by extrusion and drawing. The work has not progressed far enough to be conclusive.

Thorium Alloy Development. Suitable vacuum melting and casting equipment has been developed and a series of alloys has been cast for testing workability, corrosion behavior, and mechanical properties. Tensile tests of thorium specimens have confirmed the existence of a yield point. The effects of various working, annealing, and alloying treatments on the presence of the yield point are being investigated.

Impact Testing of Thorium. Charpy impact tests at temperatures from -196°C to 280°C are being conducted. The results will be used to determine the existence of transition temperatures.

Materials Testing Reactor Fuel Assemblies. Efforts to reduce the number of operations in the brazing procedure for fuel assemblies have indicated that the assembly must be thoroughly dried (four hours at 150°C) prior to the brazing.

[redacted]

T

Bonding Uranium to Other Metals. Experiments have been started to bond to uranium a metal which has good strength and heat conductivity. Silver has been applied to flat uranium specimens by plating, amalgamation with mercury and by bonding with some other metal foil, such as tin. The plated specimens were then rolled to produce a metallurgical bond. Bonds which could not be pried apart by a spatula after being clamped in a vise at a temperature of 220°C have been obtained between silver plated uranium and silver plated copper by mercury amalgamation or with tin foil between the two. Work is in progress to determine the optimum condition for the best bond.

Preferred Orientation and Anistrophy in Properties of Metals. The method for determining the type and degree of preferred orientation using an X-ray diffraction goniometer and a spherical specimen, has been applied to a comprehensive investigation of a sample of alpha-extruded uranium. The data thus far obtained from the four foot extrusion indicates that the preferred orientation may be described as a duplex fiber texture, the preferred directions in the grains being either [010] or [410]. Axially these crystallographic directions align parallel to the extrusion direction. Away from the axis, they are inclined to the extrusion direction with the apex of the cone so described to the front end of the bar. When more data are obtained from this rod and other extrusions, a knowledge of the preferred orientation should be had which will reveal the mechanisms of deformation and recrystallization in uranium.

Mechanical Properties of Metals. The installation of the creep laboratory is progressing and the rest of the machines should be delivered by the middle of September. The deformation work on copper has been completed and the data are being correlated with the strain-stress-time hypothesis.

Static Corrosion Testing. A series of stainless steels were corrosion tested in 1000°C lithium for four and 40 hours. Preliminary data indicate a tendency of the ferritic iron-chromium alloys to be somewhat more resistant to attack than the austenitic alloys, but the evidence is as yet insufficient to warrant recommendation of the ferritic stainless steels as container materials.

Forty-hour tests on pure metals and selected high temperature alloys in lithium tend to confirn the results of the four-hour tests. Iron, zirconium, molybdenum, tungsten, tantalum and columbium show good resistance to 1000°C lithium.

A few metals have been tested in bismuth-2% uranium and lead-2% uranium alloy baths. Preliminary results show substantial attack on most metals tested, with films formed in most cases. Molybdenum and columbium appear to be the most suitable for containing these alloys on the basis of the incomplete data. The testing of various materials in 1000°C sodium hydroxide has as yet been inconclusive because of the impurity of obtainable NaOH.

Circulating Corrosion Testing. Thermal convection loops are being fabricated from a variety of tubing for testing with lithium and sodium at 1000°C.

Effect of Neutron Irradiation on Copper Alloys. Electrical resistance measurements indicate that there is a difference in the rate of gamma phase precipitation between irradiated and non-irradiated copper-beryllium alloy. X-ray investigation has shown a marked line broadening after irradiation, the same effect as observed on cold working.

As copper-aluminum alloys change resistance in a manner contrary to that of other systems during irradiation, experiments are being carried out to explain this behavior. The isothermal annealing curves of irradiated and non-irradiated Cu-Al alloys reveal that the irradiated samples partially recover their original resistance, the extent being dependent on temperature; there is the absence of a nucleation stage; the non-irradiated samples decrease in resistance dependent on temperature; there is a nucleation and growth process; for both irradiated and non-irradiated samples the resistances approach the same condition of equilibrium but from opposite directions. The response to annealing is, in the case of the non-irradiated samples, typical of a nucleation and precipitation from a super-saturated solution. The behavior of irradiated samples indicates precipitation from a super-saturated solution during irradiation followed by re-solution of the precipitate during annealing. Further experiments are planned to verify a precipitation reaction activated by irradiation.

In-Pile Creep Experiment. The apparatus for determining creep during irradiation has been completed and bench tested. It should be installed in the ORNL reactor in the very near future.

REACTOR FUEL PROBLEMS

The slug failures which have occurred in the ORNL reactor can be divided into two types: one type being weld failures, and the other failure due to diffusion between the uranium and the aluminum can. One proposed and likely solution to both problems is the use of an Al-Si alloy bond between the uranium and the aluminum can and a group of slugs so-bonded has been placed in the reactor. The main portion of the experimental work on the problem has been done on the diffusion of uranium and aluminum couples.

BONDING AND DIFFUSION IN ORNL (CLINTON) SLUGS

The 15 Al-Si bonded Clinton slugs, which have been in operation at the ORNL reactor for nine months, have not shown any evidence of irregularities as determined by visual inspection. The slugs have been operating at a maximum temperature of 330°C obtained by partial blocking of the air passage to the slug line.

All non-radiation work on the Clinton slug problem has been completed and the data are now being compiled for inclusion in a terminal report. Extensive work on the diffusion of aluminum alloys and uranium in U-Al sandwiches has been carried out and the results will be covered in the terminal report to be issued in the near future.

GASES IN BLISTERS IN MTR FUEL ELEMENTS

Additional work has been done to determine the gas causing the blisters which are formed during the annealing of the MTR fuel elements. Two analyses of the gas in the blisters have shown it to be predominantly hydrogen. There were always additional gases present due to degassing of the apparatus, but these were minor and did not prevent an exact analysis. This evidence seems to confirm the theory that the blisters are caused by water which is absorbed on the surface of the aluminum and the aluminum-uranium alloy prior to cladding and reacts when the material is annealed after the cladding operation.

THERMAL CYCLING OF HANFORD SLUGS

Cycling studies continued to show no appreciable distortion of alpha-rolled or alpha-rolled beta-heat treated uranium rod. A test rod, made from alpha-rolled uranium, was held continuously at an average center temperature of 465°C for 142 hours after it had previously been cycled 35 times. This did not produce any appreciable distortion. Another alpha-rolled rod was given a fast beta-heat treatment and subjected to 600 thermal cycles without undergoing any distortion.

Since the present data indicate that the thermal cycling produced with the thermal gradient equipment will not duplicate the distortion experienced in the Hanford reactors, the experimental work has been concluded. A terminal report will be written covering all the work on this problem.

Present Cycling Experiments. Since the effect of maintaining a constant thermal gradient in a uranium bar over a long period of time is not known, such a rod is being tested under these conditions. Test rod number 41, made from alpha-rolled uranium, was salvaged by remachining the contacts and reducing the test-section from 1.357 in. diameter to 1.098 in. diameter. The data presented in Table I indicate that no distortion had been produced in the rod when it failed from stress corrosion after 142 hours with a thermal gradient (calculated) of 385°C.

Although beta-heat treated material was not expected to produce appreciable distortion, one rod was tested in a manner similar to the tests of alpha-rolled material. A 1-5/8 in. diameter by 42 in. long alpha-rolled uranium rod was beta-heat treated by submerging the rod for 30 seconds in a lead bath at 750°C and quenching in water. A standard test rod one inch in diameter was then machined from the heat treated material. A thin copper plate was deposited on the surface, as previously described in ORNL-754.[1] The rod thus prepared, was cycled 600 times before a stress corrosion crack appeared in the test section. No distortion was apparent, (see Table I, rod No. 42).

Further work on thermal gradient cycling of uranium appears not to be justified, since no appreciable distortion has been produced.

(1) *Metallurgy Division Quarterly Progress Report for Period Ending April 30, 1950,* ORNL 754, 9 (Aug. 4, 1950).

TABLE I

Thermal Cycling of Uranium Bars

ROD NUMBER	TYPE OF MATERIAL	NUMBER OF CYCLES	LENGTH OF CYCLE (min)	END LOAD (lb)	CENTER TEMPERATURE (°C)	SURFACE TEMPERATURE (°C)	TEMPERATURE GRADIENT (°C)	AVERAGE DIAMETER, INITIAL	DIAMETER AFTER CYCLING	COOLING WATER VELOCITY (ft/sec)	CURRENT DENSITY (amps/sq in.)	POWER INPUT (kw/ft)	REMARKS
41	α rolled	0-23	20	950	465	60	405	1.3573	1.3560	38.2	13400	42.4	Arced under contacts.
		23-35	20	745	465	80	385	1.0978		32.5	14800	43.6	
		35-36	142 hr	665	465	80	385		1.0974	32.3	16600	48.9	Failed under contacts. Also developed corrosion cracks.
42	α rolled and β heat treated	0-200	20	685	310	75	235	1.0065	1.0060	30.4	15500	35.5	Small circumferential checked places, resembling the longtudinal corrosion cracks in other rods, appeared.
		200-403	20	675	305	75	230		1.0064	30.0	14700	33.5	
		403-600	20	720	300	75	225		1.0063	30.00	15500	35.3	Developed corrosion crack in test section.

EXTRUSION AND DRAWING OF URANIUM

This work is being carried out to find a more efficient way to produce natural uranium slugs. If uranium can be extruded into a rod a little larger than the required diameter and drawn to final size, it will be a more satisfactory process than the machining of rolled bar stock. Preliminary extrusion of uranium with a flat-faced die produced extruded rod without the customary barky surface normally experienced on uranium extrusions. Figure 1 shows one extruded rod made in the gamma range and Fig. 2 shows three extruded rods made in the alpha range. Extrusions attempted in the beta range were unsatisfactory, as expected. The uranium was extruded bare in all cases except for the glass that adhered to the surface from the heating bath.

The drawing operation has not been successful so far, since the uranium seizes to the drawing die. Different types of drawing compounds have been tried: Stancoat No. 1 and No. 2, Molykote, and a thin coating of copper produced by chemical replacement from a $CuSO_4$ solution. Additional work and investigation in the field of drawing compounds is necessary before large rods of uranium can be drawn.

[redacted]

PHOTO NO. Y-1920

NATURAL URANIUM EXTRUSION
Extruded through a flat faced die to 0.840 in. dia. from a 2 15/16 in. dia. x 5 in. billet. Billet heated to 900°C for 3 hrs. in glass.

Fig. 1

[redacted] PHOTO NO. Y-1942

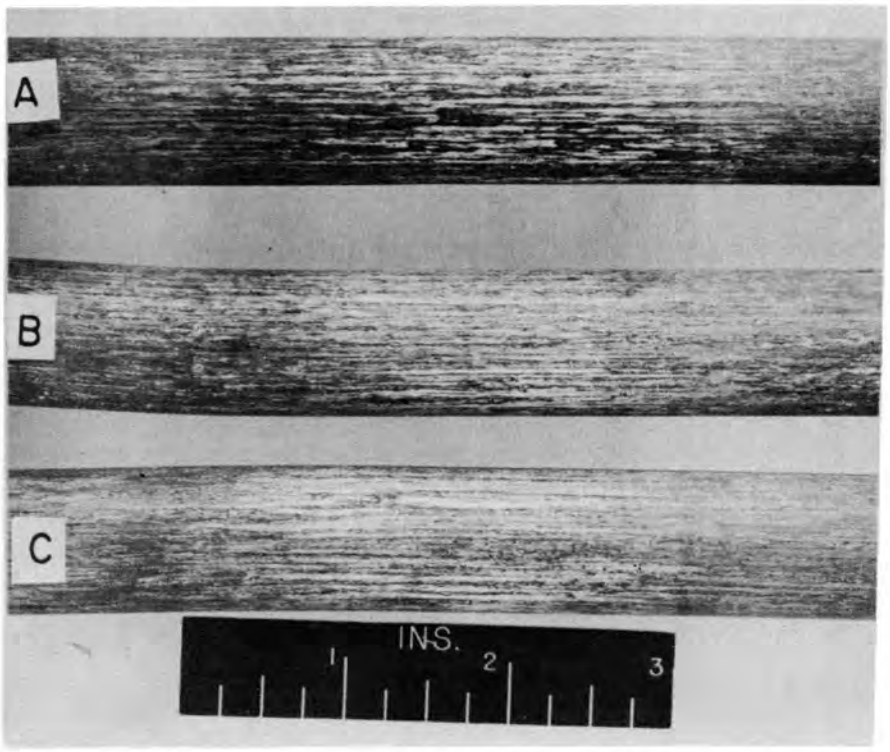

NATURAL URANIUM BARS

Fig. 2

THORIUM PROGRAM

THORIUM ALLOY DEVELOPMENT

The thorium alloy program has as its purpose the development of thorium alloys that have good corrosion resistance and good structural properties for use in reactor applications.

The first need was a furnace suited to melting and casting in vacuum; a tilting vacuum furnace was designed and is now in operation for melting and casting thorium and its alloys. Larger ingots of better quality can be made than were possible by melting and solidifying in the melting crucible.

A series of alloys, previously prepared by allowing the melt to solidify in the crucible, were cold-rolled to determine the relative workabilities of the alloys. The series consisted of alloys containing 1% to 8% of the following elements: Al, Be, In, Zr, Mn, Mg, Cr, Ti, Te, Cb, Se, Ce, and Si. It was apparent from the rolling data that the most ductile alloys were those containing Zr, Cb, Mn, Cr and Ti. The remainder of the series cracked after slight reduction.

Consequently, the first alloys melted in the tilting vacuum furnace were Zr, Cb, Mn, Ti and Cr. Corrosion test samples are being prepared from these alloys by cold-rolling into 1/8 in. plate. The ingots will also be extruded into rod for tensile test specimens.

Thorium and its alloys will be melted in a vacuum arc furnace, as well as in the vacuum induction furnace. The major drawback to vacuum arc melting is the lack of a method to produce large ingots. A device to add thorium powder to the arc furnace has been constructed to accomplish this, but has not yet been tested. The thorium powder will be melted using a water cooled electrode.

YIELD POINT OF THORIUM

In the last quarterly report[1] the appearance of a yield point in tensile tests of thorium was reported. Additional work has upheld the existence of a

(1) "Thorium Program," *Metallurgy Division Quarterly Progress Report for Period Ending April 30, 1950*, ORNL 754, 22 (Aug. 4, 1950).

yield point.

Tensile tests on Westinghouse thorium, a powder compact material made in bars ¼-in. square and 10 in. long, both in the as-received and in the annealed condition, gave a yield point in the load-elongation curve. A typical load-elongation curve for Westinghouse thorium is shown in Fig. 3. The conventional tensile test data for the powder compact thorium, Table II, shows that this material has less ductility and strength than the Ames thorium.

Compression tests on Ames thorium also show the yield point (Fig. 4). Bars of Ames thorium, 3/4 in. in diameter by 2½ in. long were compressed to a maximum load of 100,000 pounds without breaking or cracking. This represented a total change in length of approximately 80%. The average Rockwell and Vickers hardness of each compression sample was taken in the part of the specimen corresponding to the original cross section (Fig. 5). Then the hardness was determined from the edge of the original cross section to the outside of the compressed specimen. The values of average hardness and the variation of hardness from the center to the edge of the specimen are given in Table III.

Conventional sheet metal type tensile test specimens were machined from ¼-in. Ames thorium plate. After machining, the specimens were annealed at 750°C for ½ hr in a vacuum furnace. Test bars 5 and 7 were pulled in tension in the annealed condition. The yield point of thorium can be seen on the load-elongation curve (Fig. 6). Test bars 3, 6, 8 and 9 were reduced in thickness 5% by cold-rolling prior to the tensile test, and the load-elongation curves of these cold worked bars did not show the yield point of thorium (Fig. 7). The conventional tensile test data obtained from these tests are presented in Table IV. Figures 8 and 9 are photographs of the fractures of these bars.

Additional bars were cold-rolled in the same manner as tensile test bars 3, 6, 8 and 9. These test specimens are now aging at room temperature before testing to see if the aging treatment results in the return of the yield point. A load-elongation curve obtained from a bar aged at room temperature for 1250 hours did not show the return of the yield point.

Different types of samples are now in preparation. One series of samples contains alloys of Ti, Cb, and Zr. It is possible that these constituents may remove the impurities causing the yield point. A melt of Ames thorium was made in a nitrogen atmosphere in an attempt to make an alloy of high nitrogen content. A tensile specimen will be made from this high nitrogen alloy, and

DWG 9775

[redacted]

Thorium Tension Test (Wh.)

Recorder — Half Range

Load — Medium Low

Spec. No. 6

Annealed

FIG 3

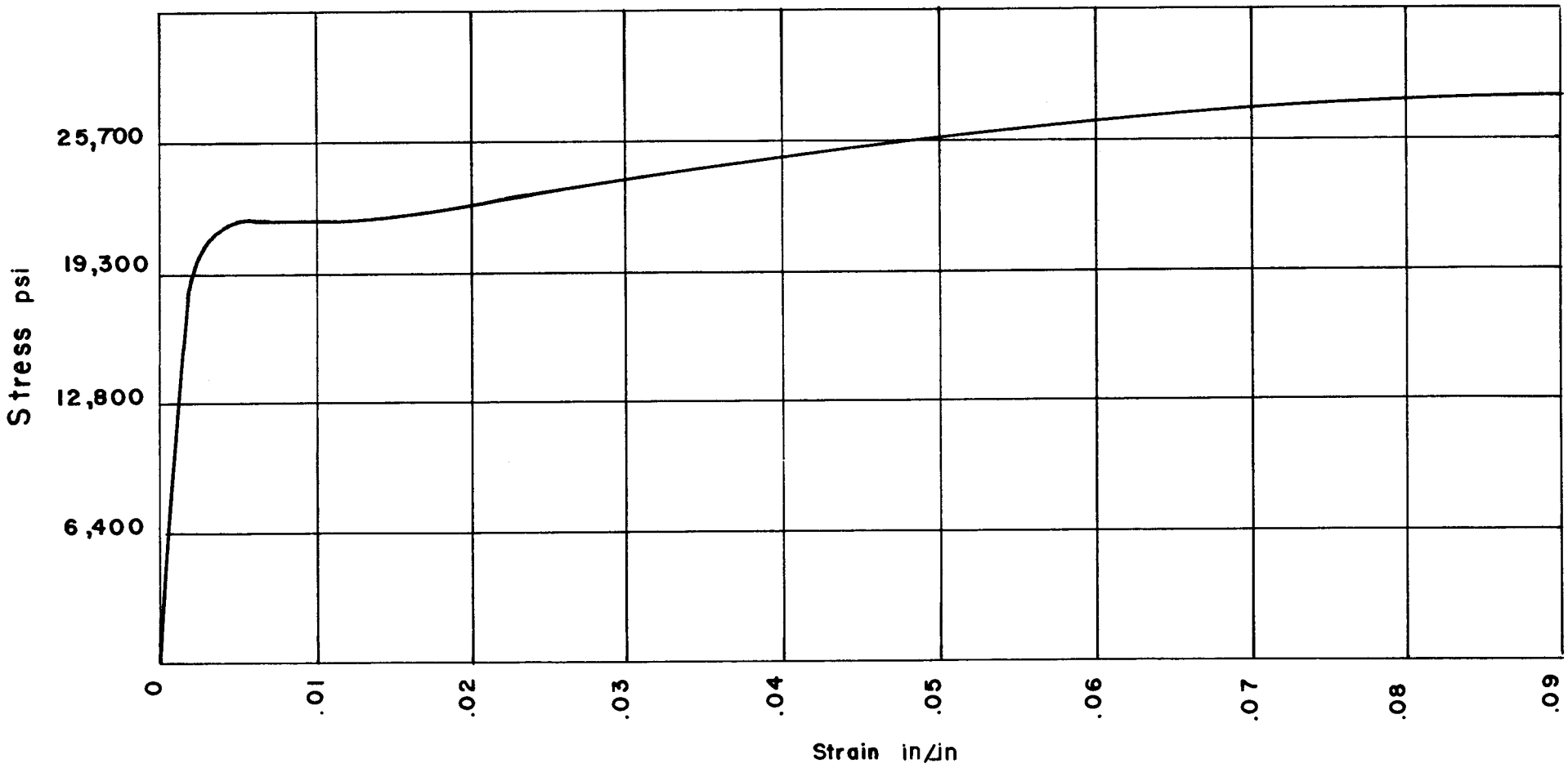

TABLE II

Westinghouse Thorium—Conventional Tensile Test Data

SPECIMEN	1	2	3	4	5	6	7
Elongation, percent in 2 in.	15	12	12	6	9	9	6
Reduction in Area, percent	7.7	13	3.6	9	9.5	6.9	16.1
Tensile Strength, psi	27,980	27,520	30,530	26,260	28,550	28,350	25,780
Ultimate Strength, psi		32,680	31,460	28,940	31,560	30,790	30,730
Proportional Limit, psi	13,270	15,632	15,160	17,510	19,560	18,300	14,320
Rockwell Hardness (B scale)	44.3	38.9	41.1	40.5	42.0	40.8	31.4
Vickers Hardness (10 kg)	86.4	83.1	83.7	91.6	88.7	89.0	70.4

NOTE: Specimens 1 - 3 were tested as received. Specimens 4 - 7 were annealed at 750°C for one-half hour before testing.

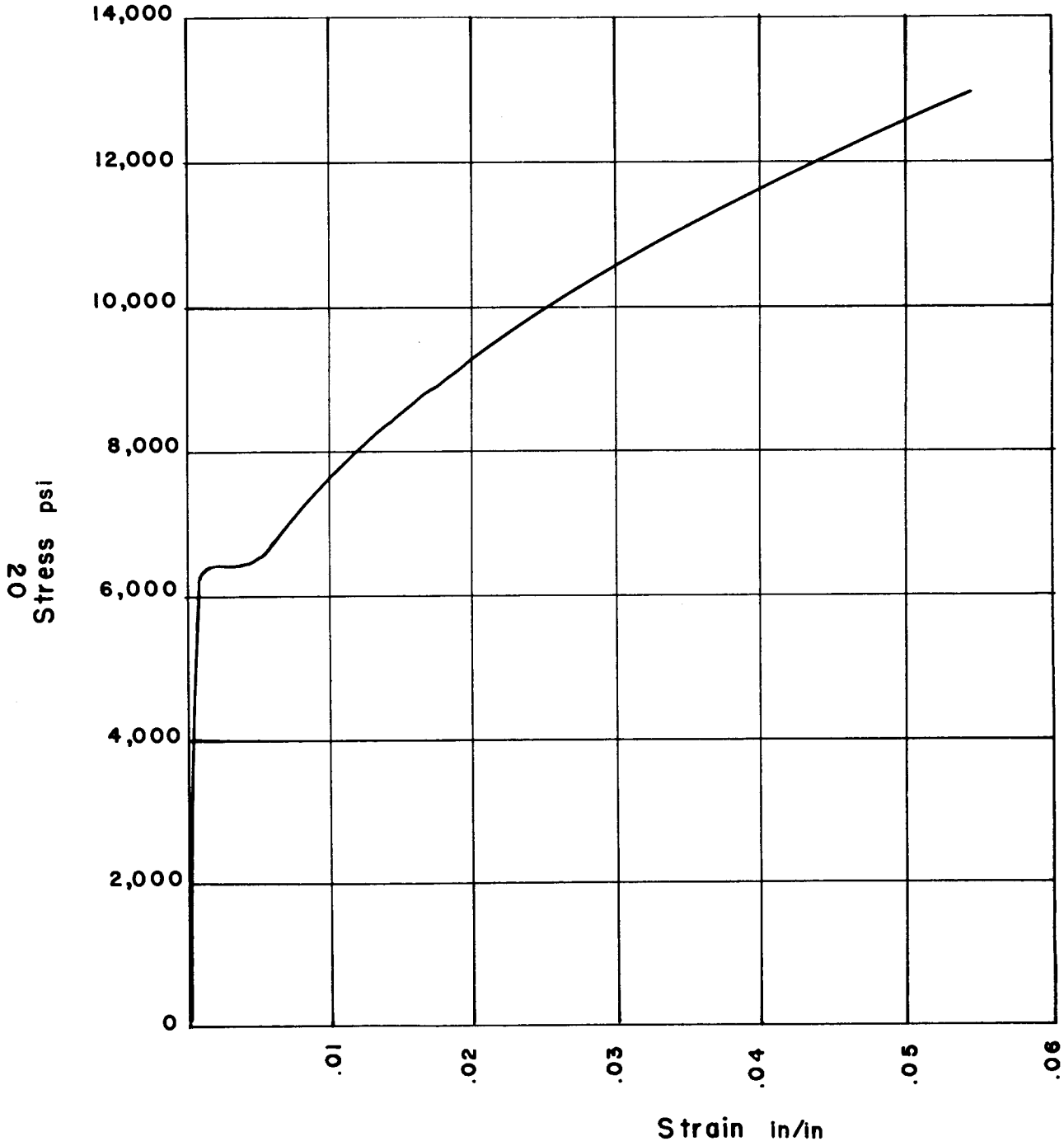

DWG 9776

[redacted]

Thorium Compression Test (Ames)

Recorder — Full Range

Load — High Range

Spec. No. 1

Annealed

FIG. 4

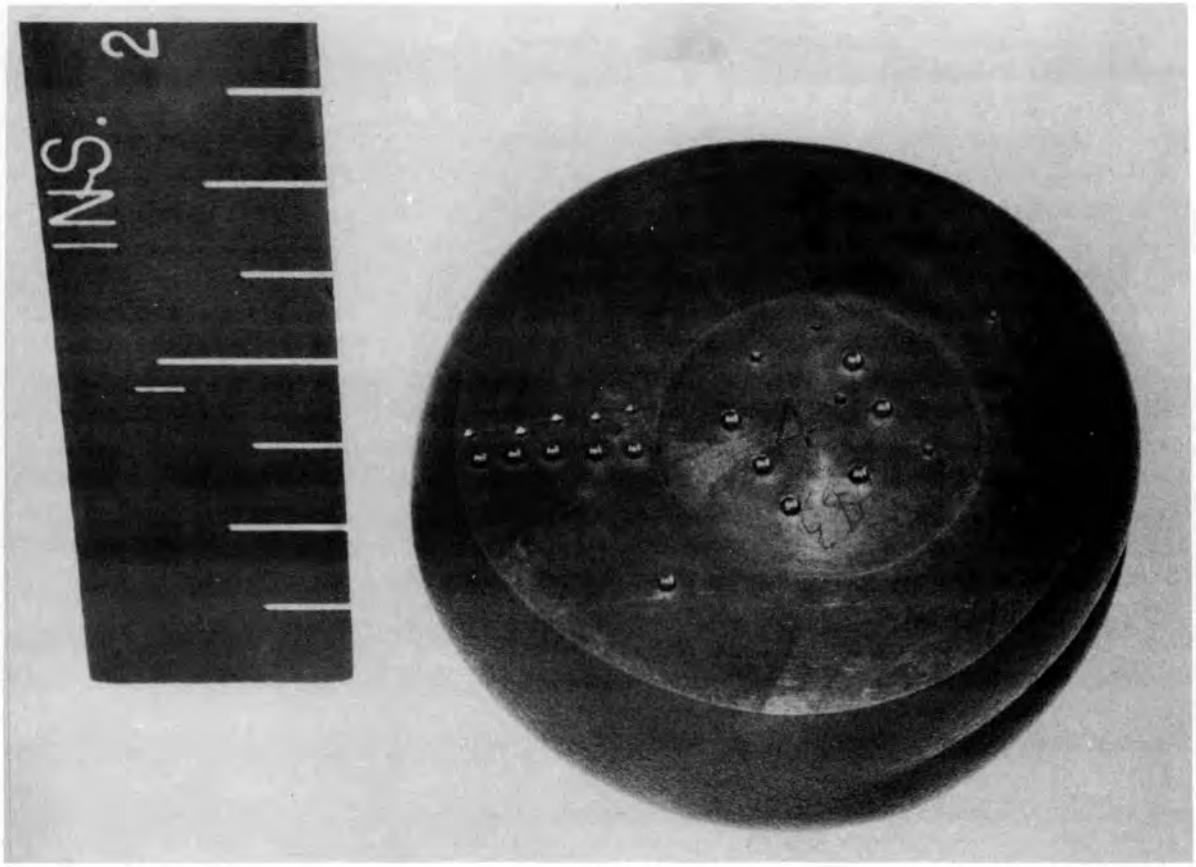

COMPRESSION SPECIMEN OF AMES THORIUM
Average Hardness found in Center of Specimen. Increasing Hardness Value from Center to outside of Specimen

Fig. 5

TABLE III

Vickers and Rockwell Hardness—Ames Compression Test Bars

AVERAGE VICKERS AND ROCKWELL HARDNESS VALUES DETERMINED FROM TEN TESTS IN THE CENTER OF THE ORIGINAL CROSS SECTION

SPECIMEN	VICKERS (10 kg)	ROCKWELL (B)
1	103	55.2
2	94.8	49.6
3	90.0	44.4
4	77.2	35.8
5	91.7	47.9

VICKERS AND ROCKWELL HARDNESS TAKEN FROM THE CENTER TO THE OUTSIDE OF THE COMPRESSED SPECIMEN

(A center - E outside)

SPECIMEN	TEST	VICKERS (10 kg)	ROCKWELL (B)
1	A	111	62.5
	B	112	65.0
	C	114	66.0
	D	116	68.0
	E	121	68.5
2	A	108	60.0
	B	110	63.0
	C	111	65.0
	D	112	67.0
	E	115	68.0
3	A	110	61.0
	B	111	62.5
	C	112	63.0
	D	114	64.0
	E	119	70.0
4	A	102	55.0
	B	103	57.0
	C	104	59.0
	D	105	61.0
	E	108	58.0
5	A	112	65.0
	B	115	67.0
	C	117	68.0
	D	119	69.0
	E	122	68.0

DWG 9777

[redacted]

Thorium Tension Test (Ames)

Recorder — Full Range

Load — Medium Low

Spec. No.5

Annealed

FIG 6

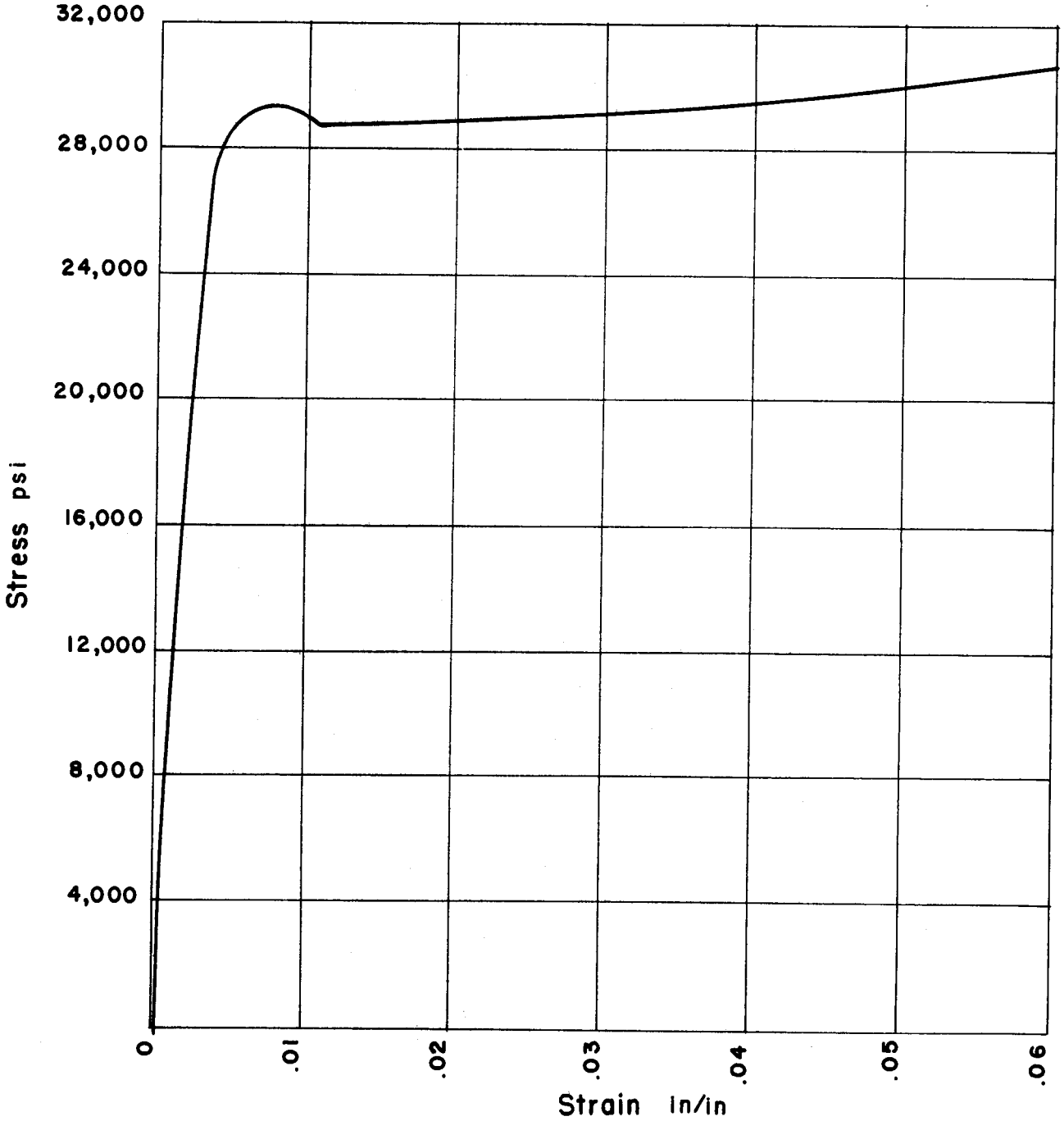

DWG 9778 [redacted]

FIG 7
Thorium Tension Test (Ames)

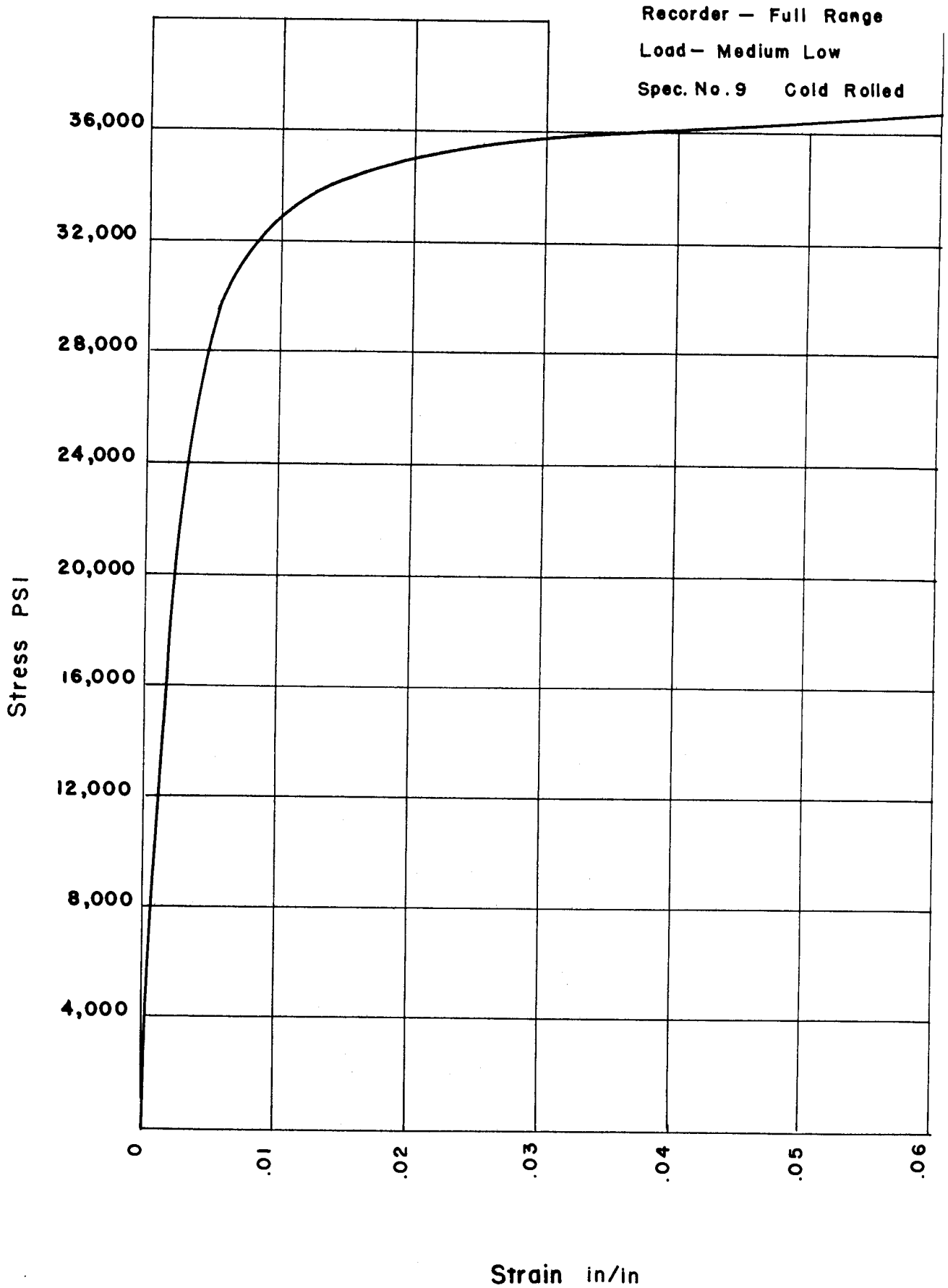

TABLE IV

Ames Thorium—Conventional Tensile Test Data

SPECIMEN	3	5	6	7	8	9
Elongation, percent in 2 in.	39.8	51.5	40.6	50	42.9	37.5
Reduction in Area, percent	60	62	61	64	60	57
Tensile Strength, psi	30,940	35,760	36,800	32,900	39,720	40,780
Ultimate Strength, psi	49,460	59,390	61,450	50,880	62,800	62,320
Proportional Limit, psi	19,210	25,614		18,700		25,614
Rockwell Hardness (B scale)	38.1	49.7	54.1	37.0	59	55.5
Vickers Hardness (10 kg)	79.4	91.5	99.0	83.1	102.3	102.3

NOTE: Specimens 5 and 7 were annealed at 750°C for one-half hour and tested. Specimens 3, 6, 8, and 9 were annealed 750°C for one-half hour then cold rolled 5%. Extensometer readings on 6 and 8 were faulty and the proportional limit could not be determined.

NOT CLASSIFIED
PHOTO NO. Y-1838

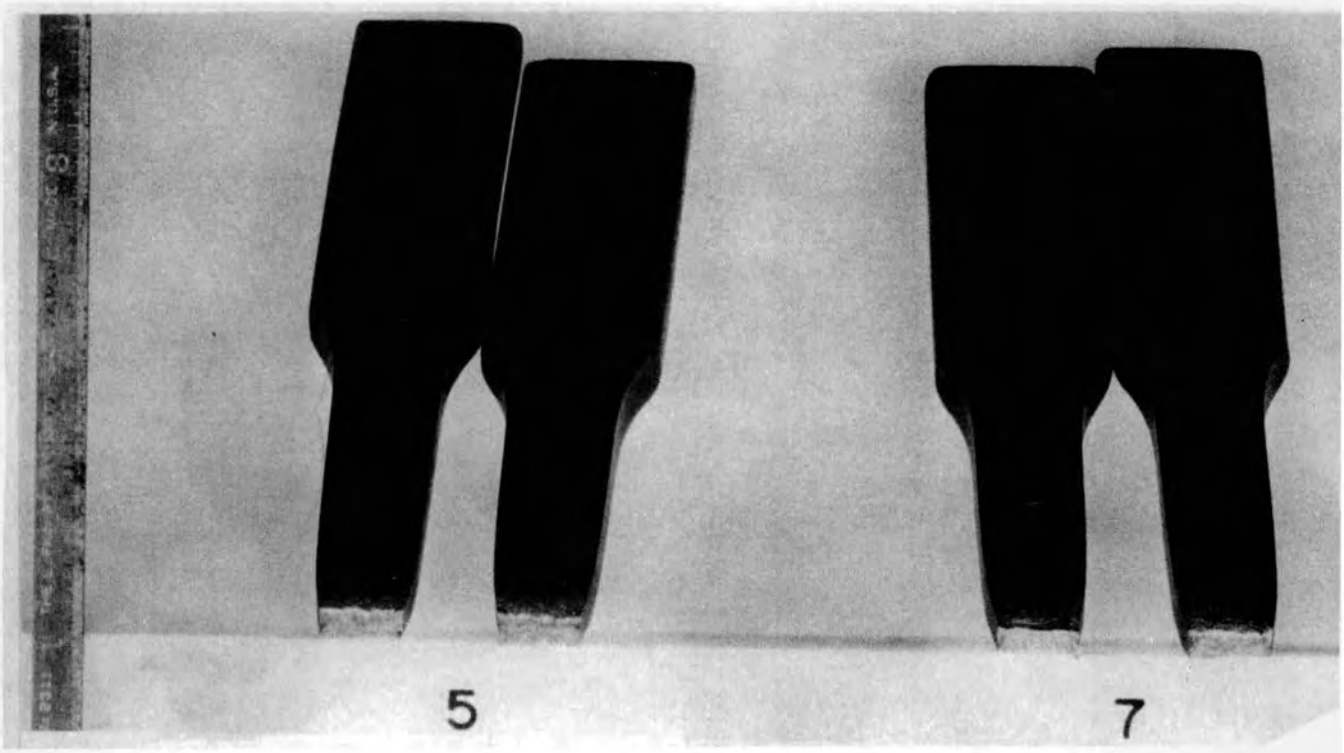

THORIUM TENSILE SPECIMENS, ANNEALED

Fig. 8

NOT CLASSIFIED
PHOTO NO. Y-1839

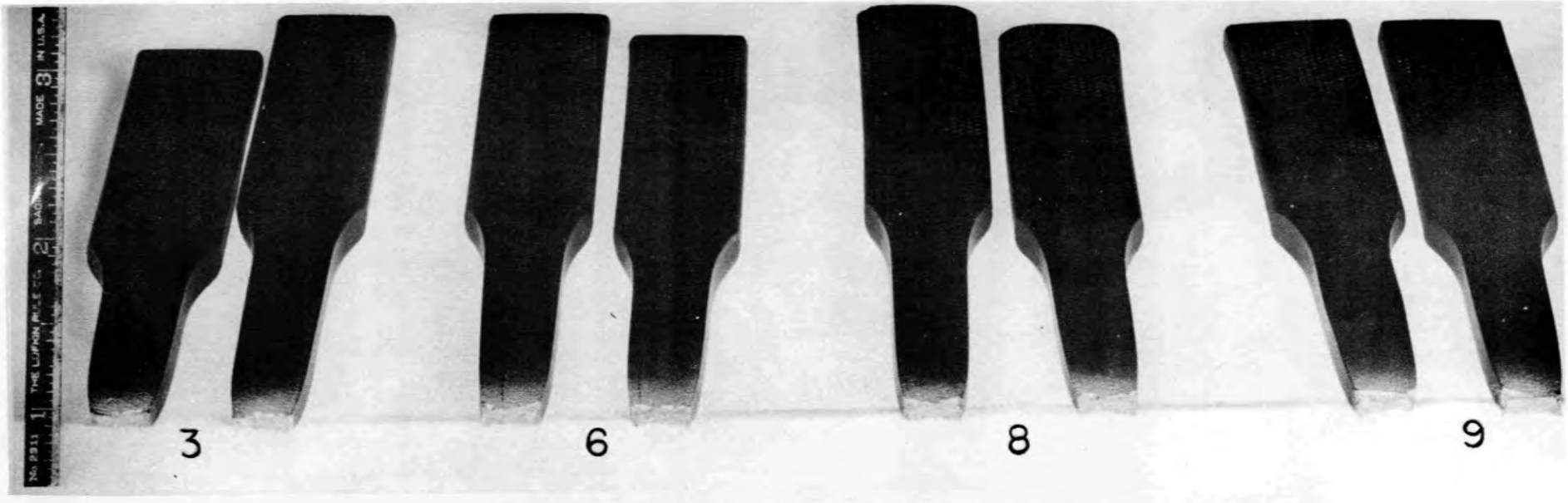

THORIUM TENSILE SPECIMENS, COLD ROLLED

Fig. 9

the appearance of the yield point in the load-elongation curve will be checked. Nitrogen is believed to be one of the primary causes of the yield point in zinc and low-carbon steels. When the results are obtained from these tests and the tests on pure thorium from the iodide decomposition process, the appearance of the yield point in thorium will be clarified.

IMPACT TESTING OF THORIUM

The impact strength of thorium was determined at the following temperatures -196°C, -80°C, 0°C, 23°C, 100°C and 280°C. The Charpy type impact specimens used were brought to the various temperatures as follows: -196°C, liquid nitrogen; -80°C, dry ice and acetone; 0°C, ice water; 23°C, room temperature; 100°C, boiling water; and 280°C, heating in oil. They were transferred from the holding container to the anvil and were broken in a very short interval of time so that the temperature of the specimens was effected only slightly before they were broken.

Table V lists the temperatures and impact strengths of the thorium. The impact strength values were plotted as a function of temperature, as shown in Fig. 10. There was considerable scatter of the data, but this is to be expected, since the samples were from different lots of thorium. Additional impact specimens are now being machined and they will be used to determine the transition temperatures for thorium, if such exist.

TABLE V

Impact Strength of Thorium

TEMPERATURE (°C)	FOOT POUNDS TO BREAK SPECIMEN		
-195.8	12.5	14.0	
- 80	18.0	11.0	
0	40.0	41.5	41.0
23	33.5	29.5	
100	31.5	43.5	38.8
280	Specimens could not be broken. (Limit of Machine 120 ft lbs).		

DWG 9779

[redacted]

Thorium Impact Test (Ames)
Charpy

FIG 10

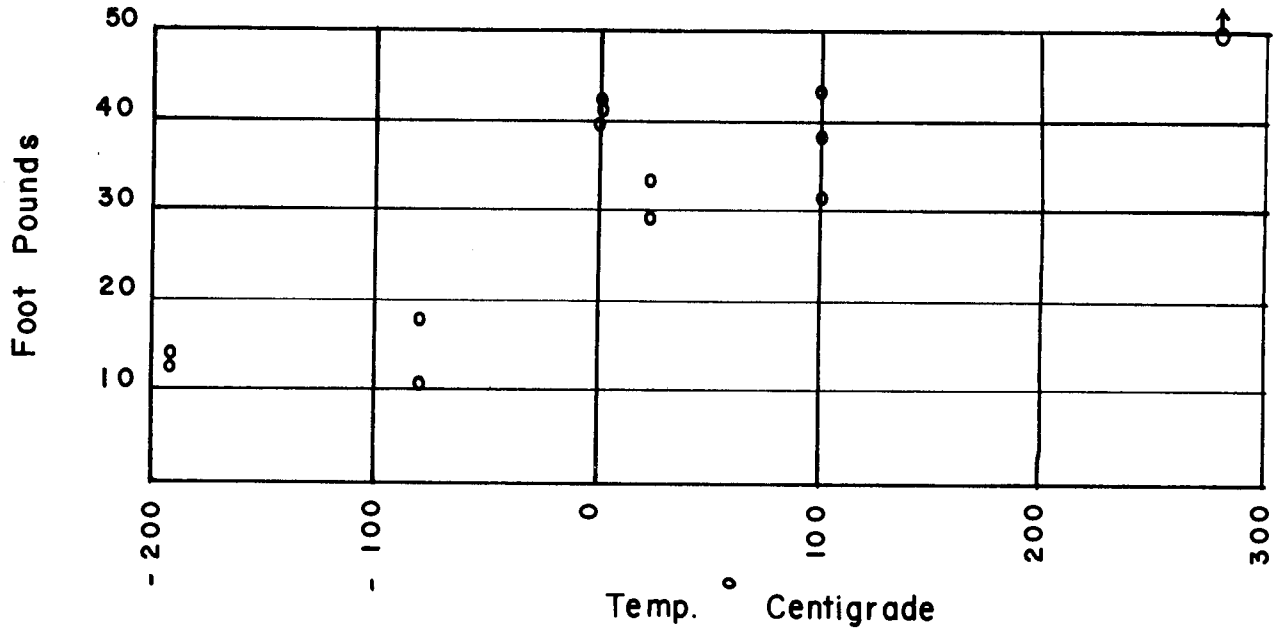

REACTOR COMPONENT ASSEMBLY FABRICATION

MATERIALS TESTING REACTOR FUEL ASSEMBLIES

MTR Fuel Sub-assemblies have, in the past, been brazed using the following sequence of operations:

1. Dry 4 hr at 150°C in stainless jig 3.000 in. wide.
2. Preheat 50 min at 850°F - ceramic jig 3.040 in. wide.
3. Braze 45 min at 1110°F - ceramic jig.

Efforts to eliminate one or both of the first two steps showed that the preheating step was unnecessary. Two runs were made in which the assembly was jigged in the ceramic jig and put immediately in the brazing furnace. Time at temperature (1110°F) was 75 min for the first, and 70 for the second assembly. Good joints were obtained. However, the plate spacing was poor and the ceramic jig cracked in both cases, indicating that the assembly must be dried thoroughly at the cold width of 3.000 in., prior to heating to brazing temperature in the wider (3.040 in.) ceramic jig.

One fuel assembly containing enriched uranium was made for an irradiation experiment at the Chalk River Reactor. Past work by the Physics of Solids group showed an increase in volume of U-Al alloy when subjected to irradiation.[1] Complete physical measurements were made on the assembly prior to irradiation. These will be compared to measurements obtained after irradiation.

A decision was made by the AEC for ORNL to fabricate the 138 assemblies for MTR start-up and to continue production at the rate of 2.3 assemblies per day until July 1, 1952. It was also decided by the MTR committee to run the MTR with a one-pass uranium cycle. After recovery of uranium from spent assemblies, it will be cycled back to isotopic separation. All assemblies will be made using new material with constant enrichment.

BULK SHIELDING FACILITY FUEL ASSEMBLIES

The Bulk Shielding Facility being built at ORNL will be powered by modified MTR fuel assemblies. A round end box will be used on the bottom of

(1) Templeton, L. C., Dismuke, S. E., and Bredig, M. A., *Radiation Stability of Uranium-Aluminum Alloys for MTR*, ORNL CF 50-4-36 (April 10, 1950).

these assemblies for positioning in the reactor. The top end will be without positioning adapters. Forty-seven assemblies are to be made as outlined in the memorandum, *Fuel Elements for Bulk Shielding Facility,* CF 50-6-132. Four kg of uranium metal were received on July 12, 1950, which, together with about 1 kg of scrap enriched U-Al alloy from the Critical Experiment will be used to fabricate these fuel elements.

BONDING URANIUM TO OTHER METALS

Efforts are being made to bond a metal which has good strength and is a good heat conductor to uranium. Copper and silver because of their high thermal conductivity are being given first consideration, followed by nickel and aluminum.

A survey was made of available literature on bonding of uranium. Keeler and Saller,[2] obtained good bonds of silver-plated uranium fuel rods inside silver-plated nickel tubes by amalgamating the mating surfaces with mercury, then drawing and heating. A visit was made to Battelle Memorial Institute to discuss this report and the plating and solid phase bonding of uranium.

Los Alamos[3] successfully silver-plated ½-in. rod which was subsequently swaged and drawn to 0.005 in. wire with a uniform silver coating. Cast uranium plates were plated with 0.003 in. silver and rolled without failure of the plating.[4]

Samples approximately 2 in. × ¾ in. × 1/8 in. were sheared from 2 in. × 1/8 in. rolled strip, and silver plated by the procedure reported in BMI T-6.[5] At 20X magnification the plating on the 2 in. × ¾ in. face was coarse, and small holes, not quite through the plating to the base, were frequent. On the rough edges resulting from shearing, grooves through the plating to the uranium base were frequent. Silver plating, 0.003 in. thick, will not stand heating in air at 300°C for one hour. Oxidation of uranium occurs through grooves in sides of specimens and oxidation easily progresses under the loosely adhering 2 in. × ¾ in. plated surface. Blistering also occurs as an oxide, resulting from diffusion of oxygen through small holes in the plating, forcing up the plating.

Amalgamating the entire plated surface with mercury did not result in improvement of ability to withstand heating in air.

(2) Saller, H. A. and Keeler, J. R., *The Bonding of Uranium to Nickel,* BMI-T-6 (Feb. 1, 1949).

(3) Anderson, R. E., Taub, J. M., and Doll, D. T., *Fabrication of Uranium Wire,* LAMS-967 (Oct. 25, 1949).

(4) Edelman, R. E. and Lamb, J. M., *Fabrication of U^{235} Discs for the General Electric Power Pile,* LA-720 (Dec. 29, 1948).

(5) Saller, H. A. and Keeler, J. R., *op cit.,* BMI-T-6.

Vacuum annealing at 600°C for one hour following plating did not improve the ability of the uranium to withstand heating to 350°C in air.

Cold reduction of 0.002 in. given to plated specimen resulted in good adhesion of silver plate to uranium when heated in air at 350°C for three hours. Blistering on the 2 in. × ¾ in. surface was not reduced, but adherence where not blistered was good and progressive attack from the edges exposed by poor plating was held down. Vacuum annealing at 600°C for one hour combined with cold-rolling did not improve the results, nor did the use of argon atmosphere in a muffle furnace.

Cold reduction of 0.002 in. applied to plated specimen, followed by an additional 0.003 in. plate and a 0.001 in. reduction, greatly reduced porosity blisters on the 2 in. × ¾ in. surface and reduced cracking at the edges.

As a result of the visit to Battelle, better plating results are expected in the future. Surface preparation of uranium will be improved by machining. Thicker silver plating and burnishing will be used in an effort to reduce oxidation of uranium.

One surface of a 2 in. × ¾ in. × 1/8 in. piece of 0.003 in. silverplated uranium, reduced 0.002 in. by rolling, was amalgamated with mercury on one side and pressed to a ½-in. square piece of silver which had been amalgamated with silver. A small vise was used to apply pressure and the vise and specimen were heated in air at 350°C for four hours. The resulting bond was metallographically good except that oxides remained at the original surface. Silver plating in unbonded areas was almost wholly removed from the uranium specimen (Fig. 11).

Four compacts were made by pressing 0.003 in. silver plated uranium samples to ½-in. square silver samples with a piece of 0.002 - 0.004 in. tin foil sandwiched between. The four vises containing these specimens were placed in a drying oven at 220°C and removed at one-hour intervals. There was no bond and little evidence of diffusion in the specimen after one hour. The two-hour and three-hour specimens showed evidence of diffusion but were easily separated. The four-hour specimen could not be pried apart with a spatula. Metallographically, the bond appeared sound. Silver-tin compound formation may be seen at each side of the tin in Fig. 12.

[redacted]

PHOTO NO. Y-1954

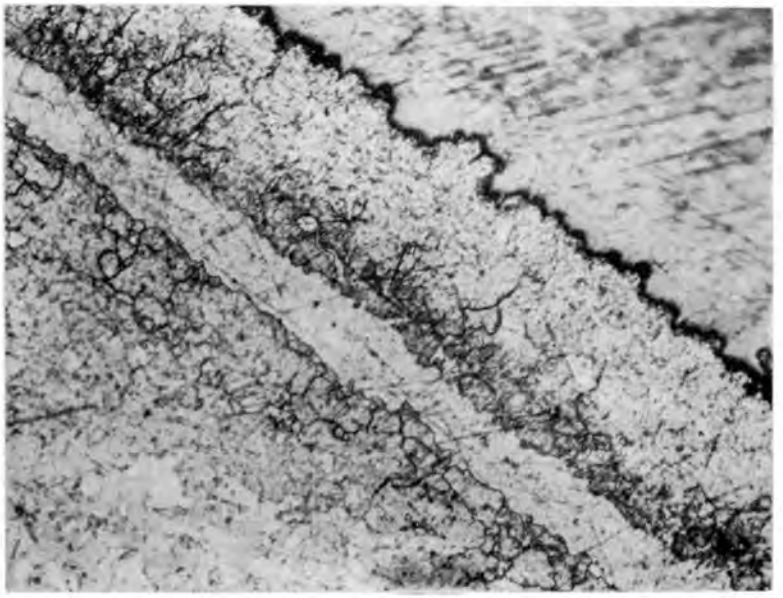

Silver Bonded to Silver Plated Uranium by Mercury Amalgam.

Fig. 11

PHOTO NO. Y-1957

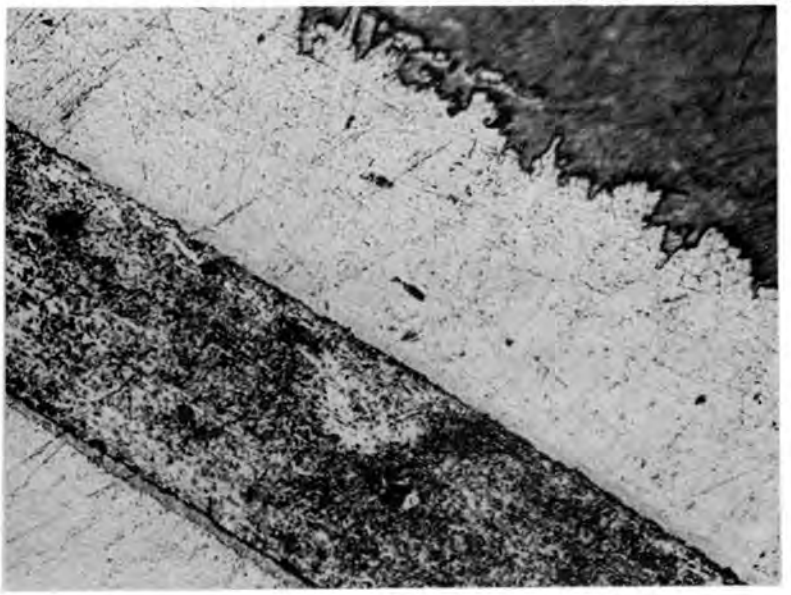

Silver Bonded to Silver Plated Uranium by Tin.

Fig. 12

Bonds of sufficient strength not to be pried apart by a spatula have been attained between silver-plated uranium and silver-plated copper by mercury amalgamation or with tin foil between. Work is being done to determine the optimum conditions for producing the best bond.

LEAD CREEP FOR MTR NEUTRON WINDOW

During this period a preliminary memorandum was issued to provide estimated engineering design data. At the time of issuance of this memorandum the average period of stress was 1900 hrs. This has now been increased to 3200 hrs.

In the 1900 hr period, a stress of 30 psi and a temperature of 150°C showed no marked elongation of any of the samples. At 3200 hrs the overall elongation rate for the specimen showing maximum elongation was still less than 0.001 in./in./year. This figure includes the effect of any non-axial loading and the deformation during the first or rapid stage of creep.

With 60 psi and 150°C after 1900 hr the average elongation rate was reported as 0.0011 in./in./year for chemical lead and 0.0017 for calcium lead. The present rates average 0.0012 and 0.0015 in./in./year, respectively.

Additional specimens are now being tested at 120°C and 180°C with stresses of 30, 45, 60 and 90 psi as well as some confirmation tests at 150°C. After more than 500 hrs these specimens are still in the initial stage of creep. A long time creep rate cannot be determined until they have entered the second stage so this figure will be given in a later report.

PREFERRED ORIENTATION AND ANISOTROPY IN PROPERTIES OF METALS

In a previous report[1] a new method was described for accurate determination of type and degree of preferred orientation using a Geiger counter X-ray diffraction goniometer. The unique feature of this method is that a spherical diffraction specimen is employed, permitting complete and quantitative examination of the preferred orientation with one specimen and without resort to complicated corrections for variations in diffracting volume and focusing.

Employing this method, a rather comprehensive investigation has been made of a sample of α-extruded uranium. A four-foot length of 1½ in. diameter bar was extruded through a conical die at 500°C billet temperature from a 3-1/8-in. diameter ingot (extrusion ratio 4.3). The extruded rod was water-spray quenched as it emerged from the die to retain, insofar as possible, the as-extruded structure. The photomicrographs of Fig. 13 depict the deformed grain structure of this rod—there is no evidence of any recrystallization.

A sample was taken from the middle of the extruded length, and three diffraction specimens were machined from this sample, as illustrated in Fig. 14. The spherical surfaces of the specimens were lapped to smoothness and then electropolished to remove the surface layers deformed by machining and lapping (the specimens were reduced in diameter approximately 0.010 in. by electropolishing).

Examination was made on a Norelco Type 12021 Geiger counter X-ray diffraction goniometer with Cu Kα radiation. The specimens were rotated (at 200 rpm) about their longitudinal axes continuously during the exposure.

Plots of the intensity of diffraction vs. the angle, ϕ, between the extrusion direction and the normal to the diffracting plane for the various planes for each specimen are given in Figs. 15 to 24. In these plots, intensities at different points on the same curve are quantitatively comparable and indicative of the proportion of the diffracting volume having that plane in the proper orientation for diffraction. Intensities on different curves,

(1) "Studies of the Properties of Uranium and Other Pure Metals," *Metallurgy Division Quarterly Progress Report for Period Ending January 31, 1950*, ORNL 583, 37 (Mar. 10, 1950).

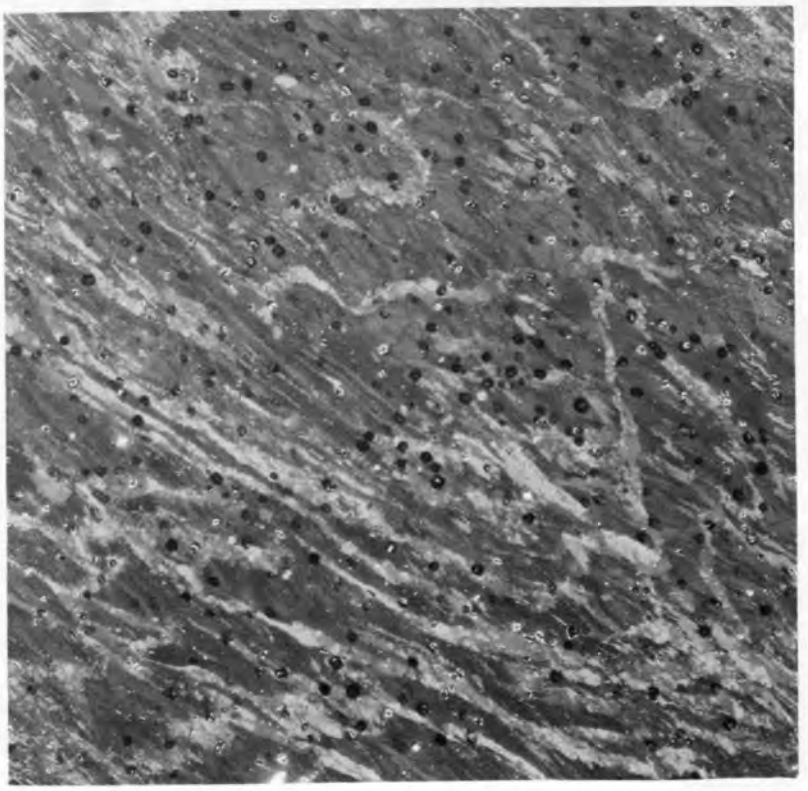

NOT CLASSIFIE

PHOTO NO. Y-1
M. Spec. – 780– E
Long.

Mag. – 150 X

Etch – Pol. Lt.

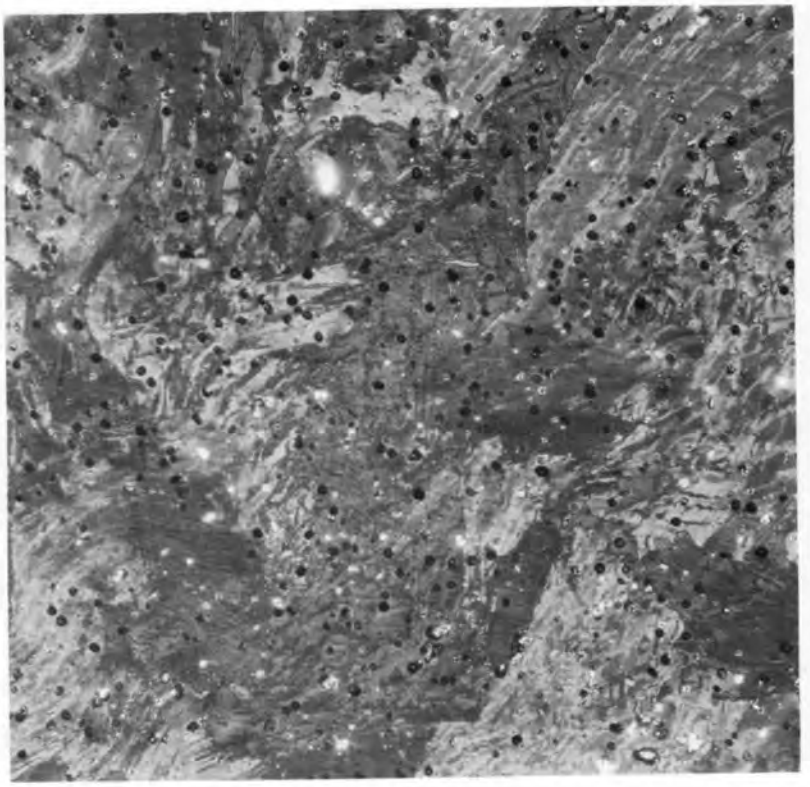

PHOTO NO. Y-1
M. Spec. – 780–
Transv.

Photomicrographs Showing the Deformed Grain Structure of the Sample of α-extruded Uranium from Which the X-ray Diffraction Specimens Were Machined

Fig. 13

DWG.-9754

[redacted]

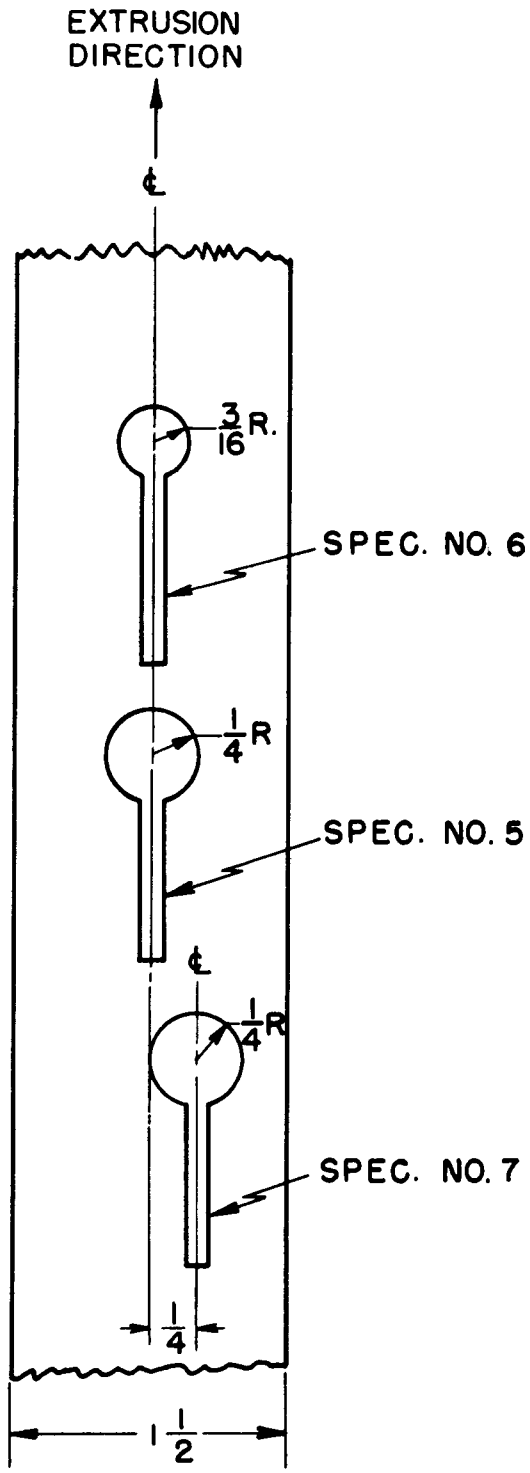

FIG. 14

SKETCH SHOWING THE DIMENSIONS OF THE X-RAY DIFFRACTION SPECIMENS AND THE LOCATIONS IN THE SAMPLE OF α-EXTRUDED URANIUM FROM WHICH THEY WERE MACHINED.

DWG. 9755

[redacted]

FIG. 15

PREFERRED ORIENTATION PLOT – (110)-α - EXTRUDED URANIUM

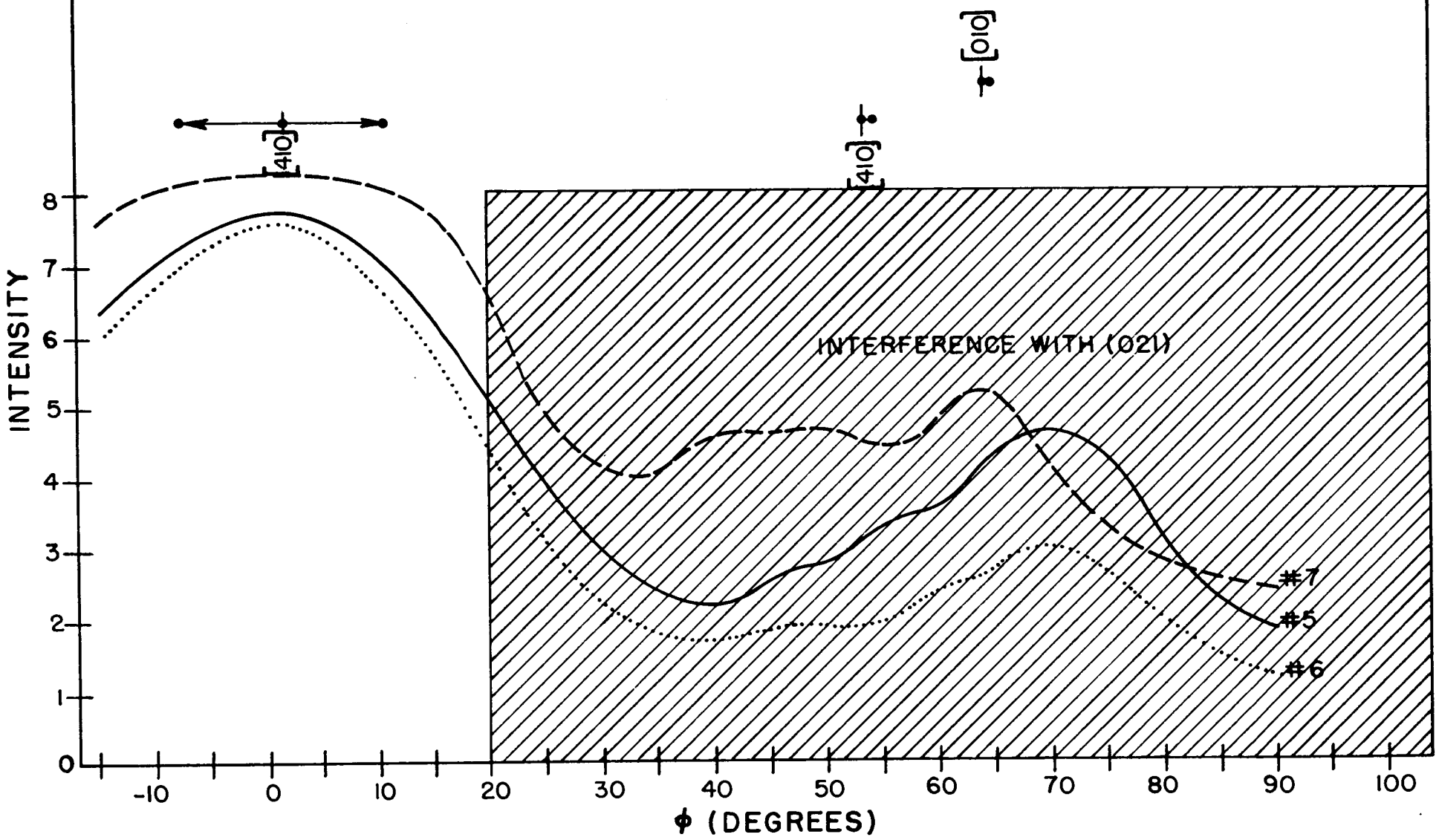

DWG. 9756

[redacted]

FIG. 16
PREFERRED ORIENTATION PLOT—(021)-α-EXTRUDED URANIUM

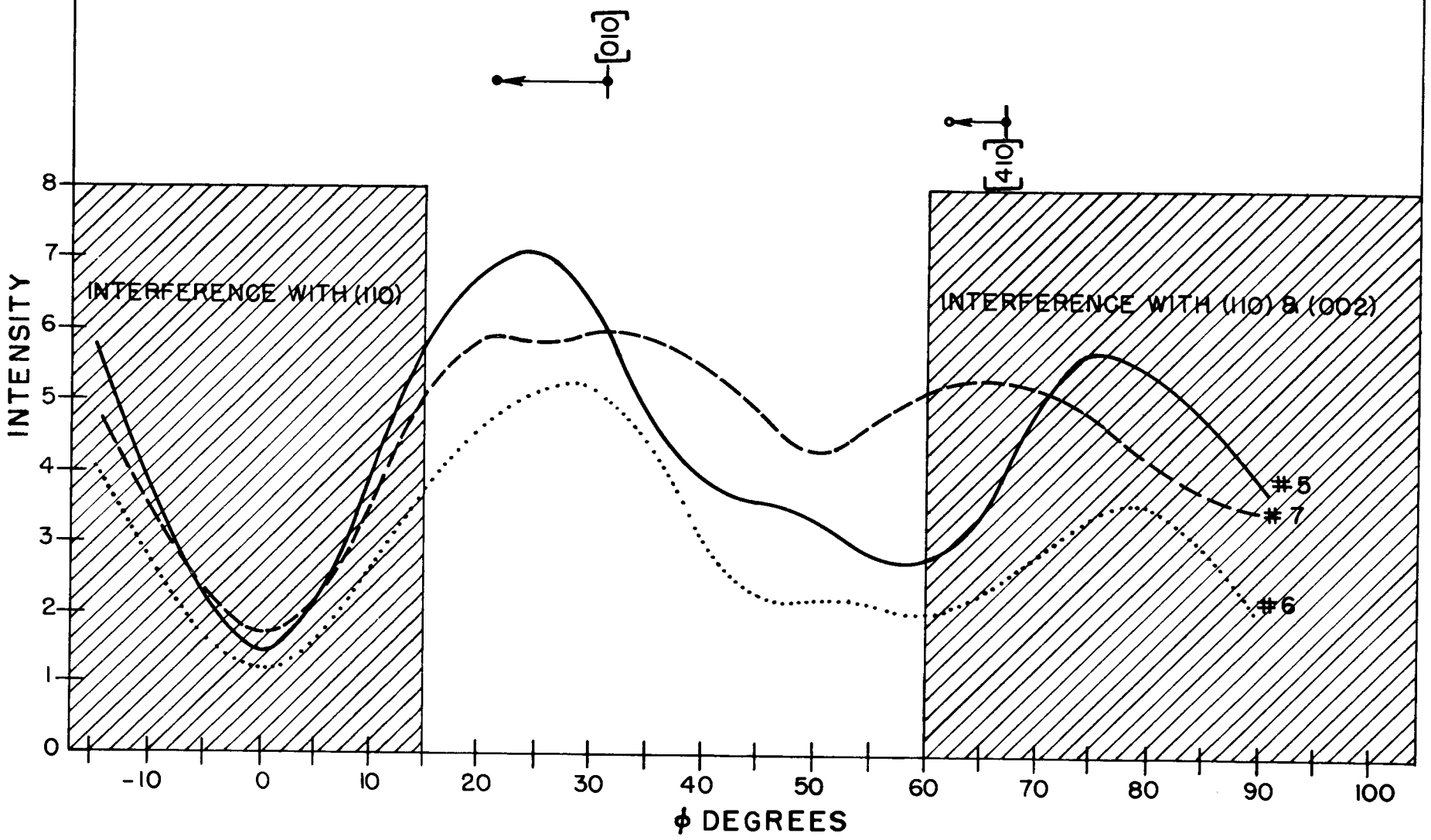

DWG. 9757

[redacted]

FIG. 17

PREFERRED ORIENTATION PLOT—(002)—α-EXTRUDED URANIUM

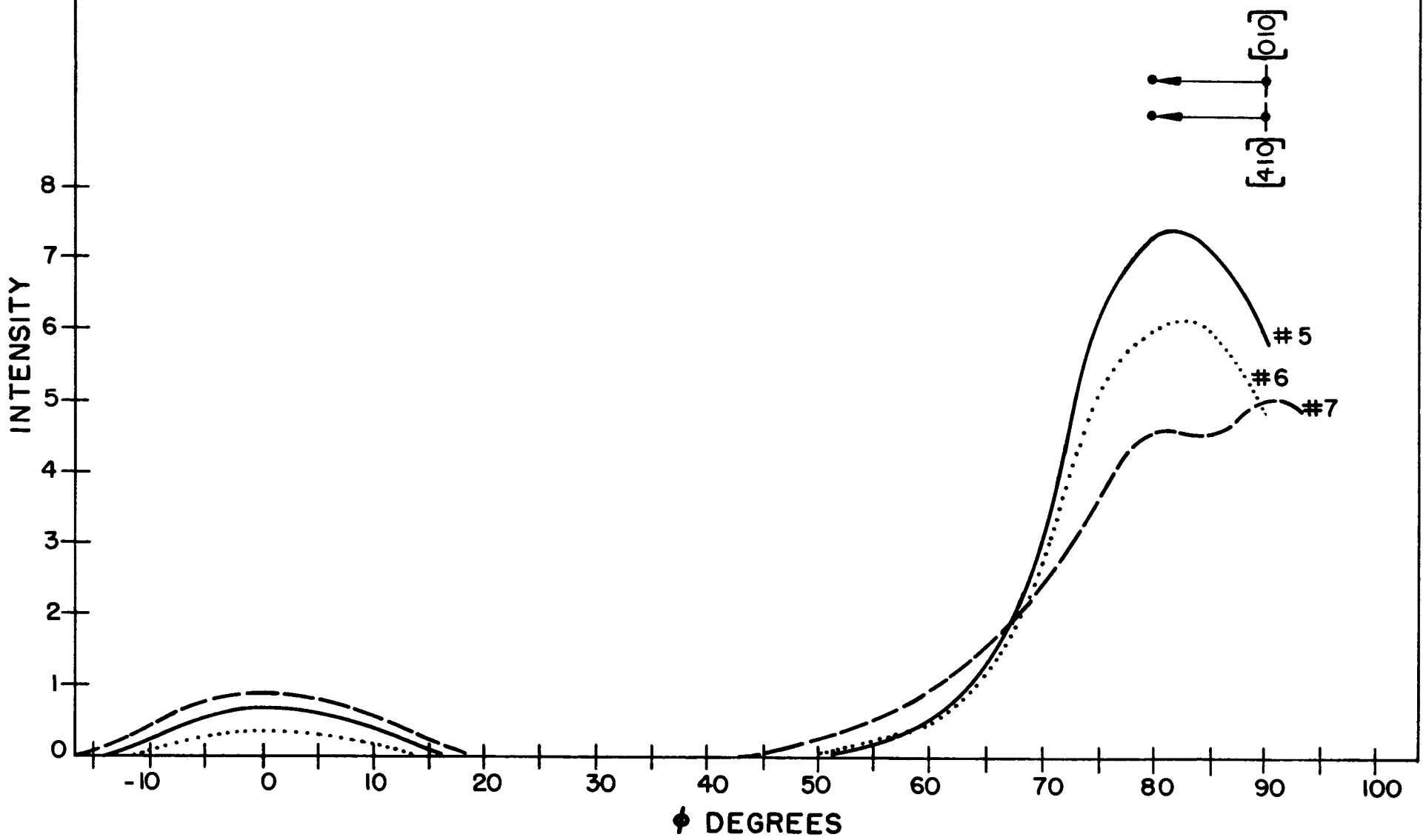

DWG. 9758 [redacted]

FIG. 18

PREFERRED ORIENTATION PLOT — (111) — α - EXTRUDED URANIUM

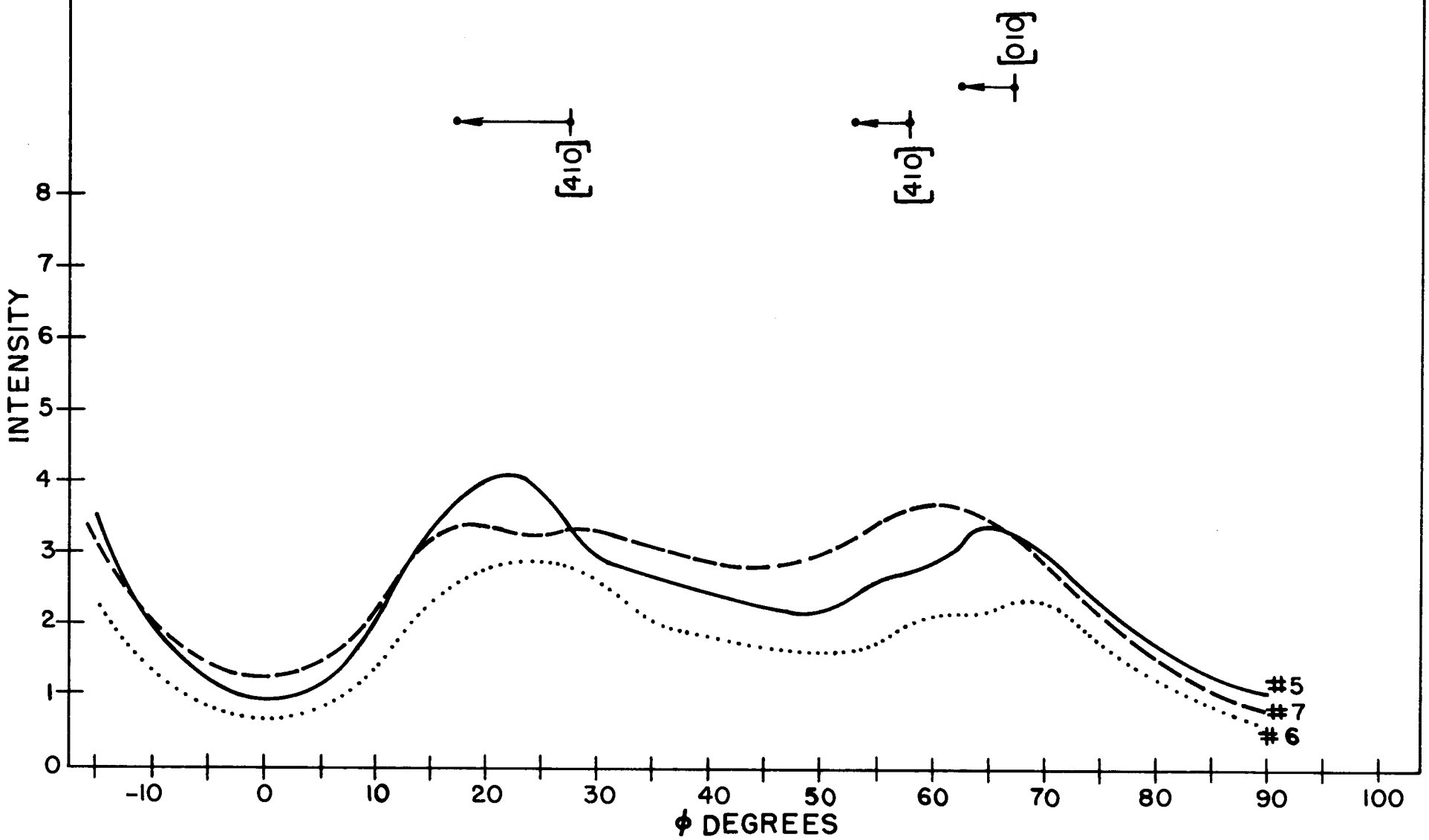

P-41

DWG. 9759

[redacted]

FIG. 19

PREFERRED ORIENTATION PLOT – (112) – α – EXTRUDED URANIUM

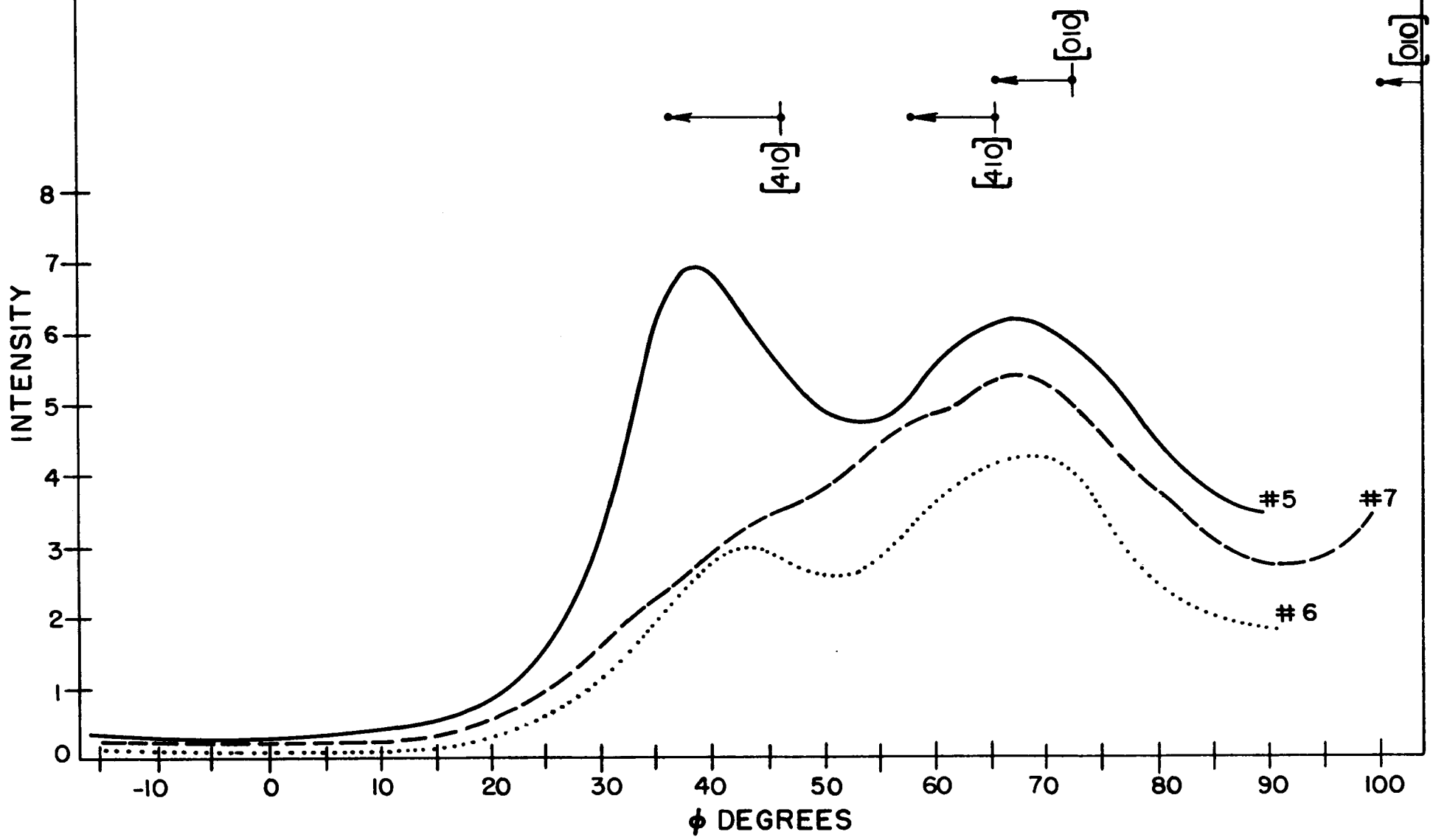

P-42

DWG. 9760 [redacted]

FIG. 20

PREFERRED ORIENTATION PLOT - (131) - α - EXTRUDED URANIUM

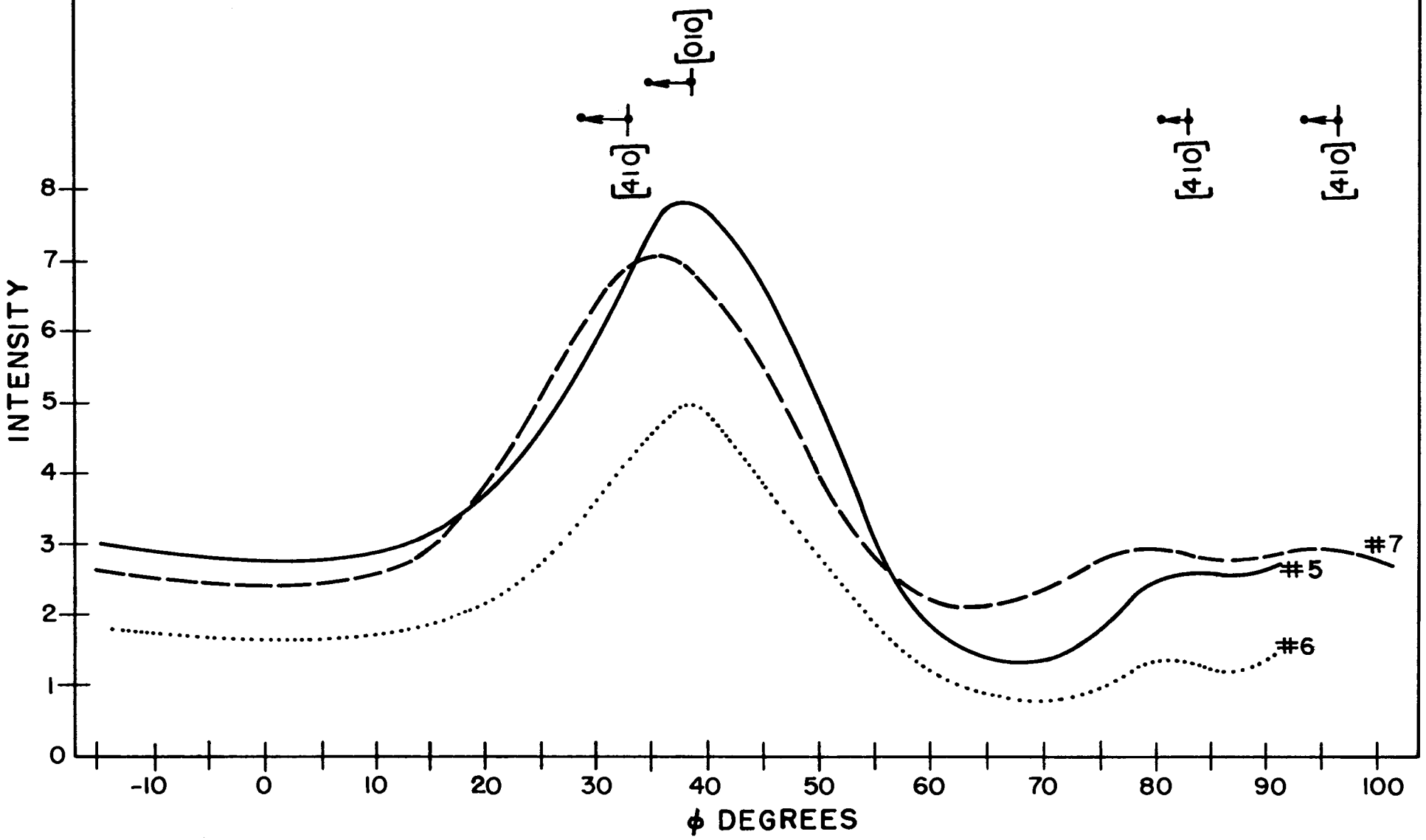

DWG. 9761

[redacted]

FIG. 21

PREFERRED ORIENTATION PLOT - (040) - α - EXTRUDED URANIUM

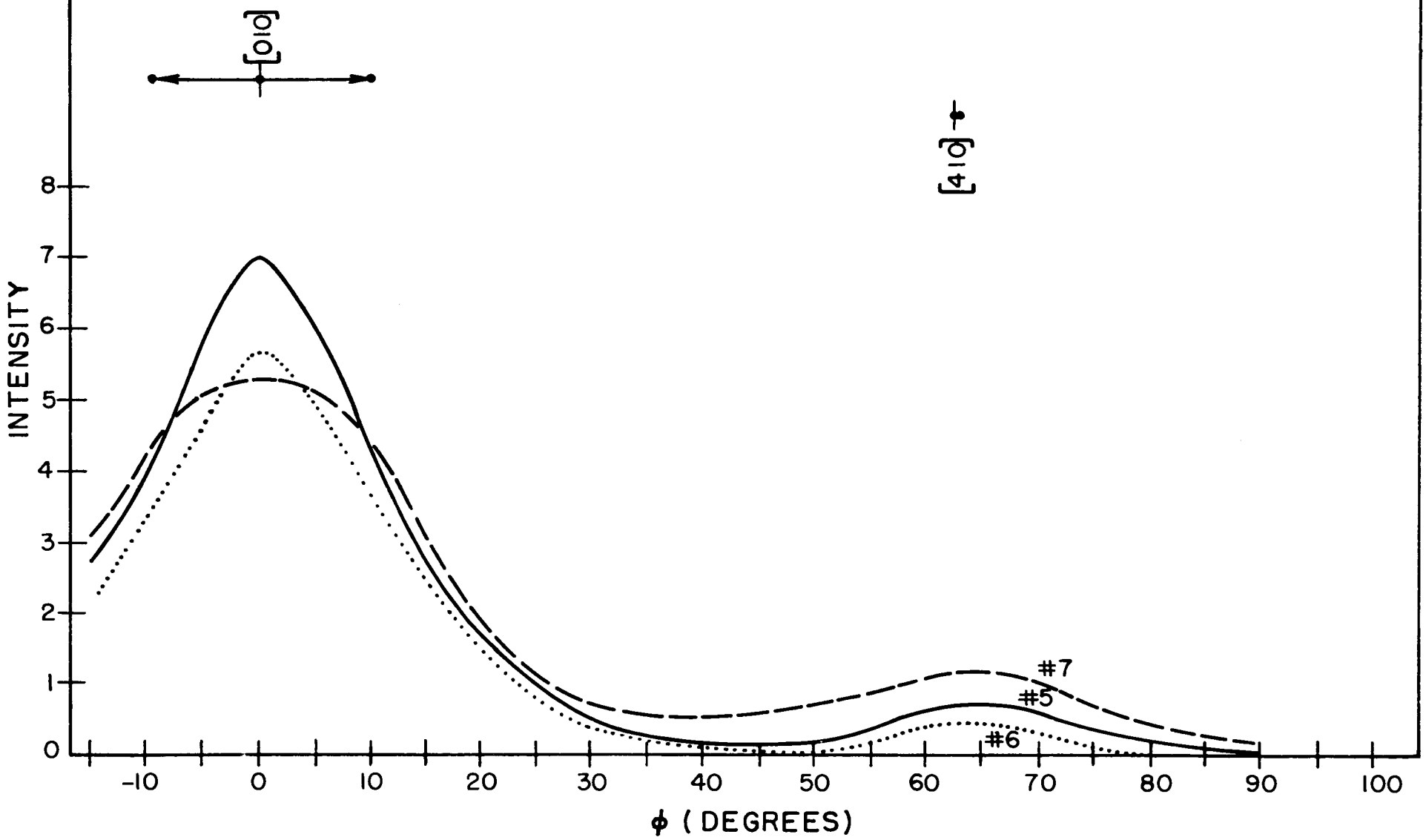

DWG. 9762 [redacted]

FIG. 22

PREFERRED ORIENTATION PLOT – (023) – α – EXTRUDED URANIUM

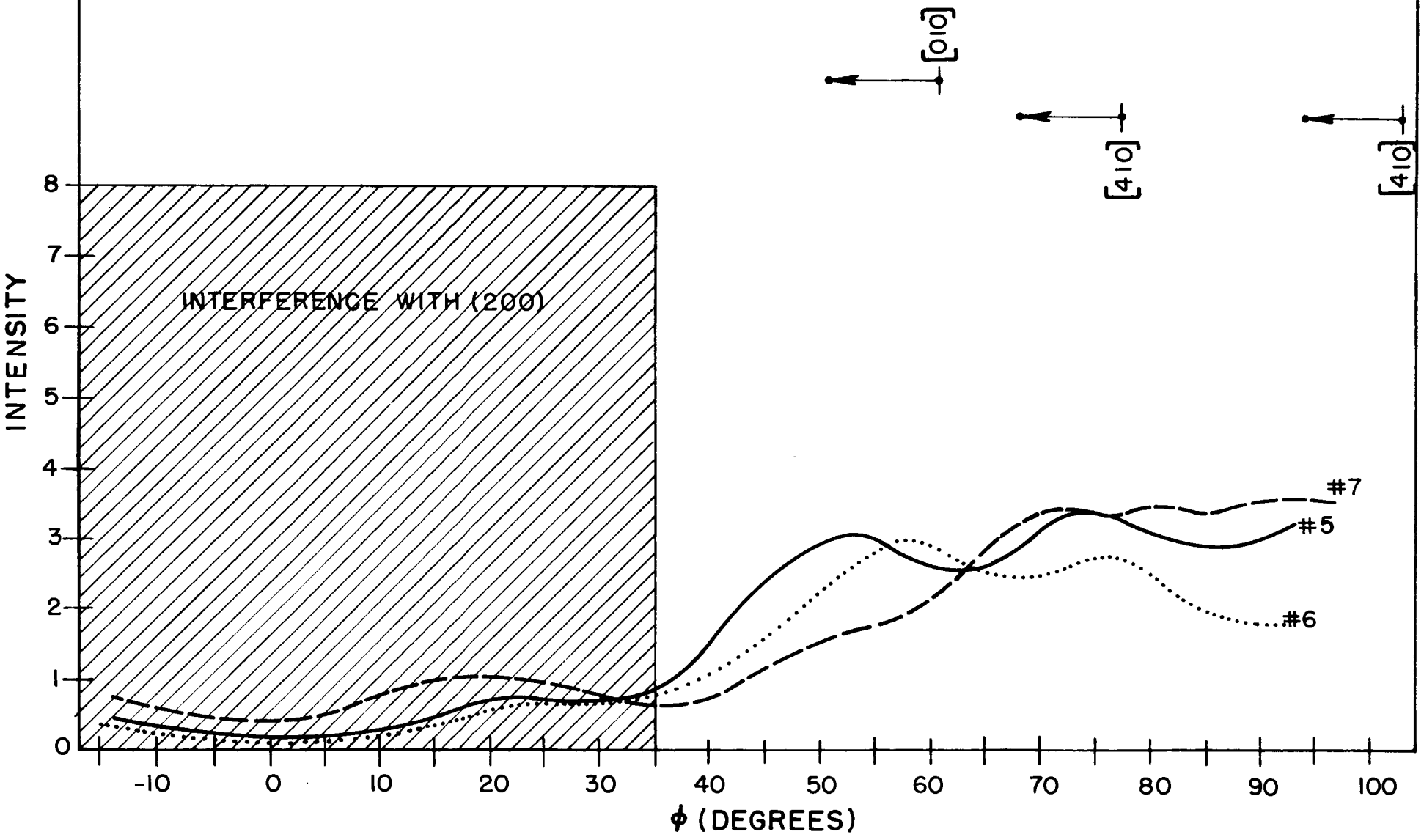

DWG. 9763

[redacted]

FIG. 23

PREFERRED ORIENTATION PLOT -(200) - α - EXTRUDED URANIUM

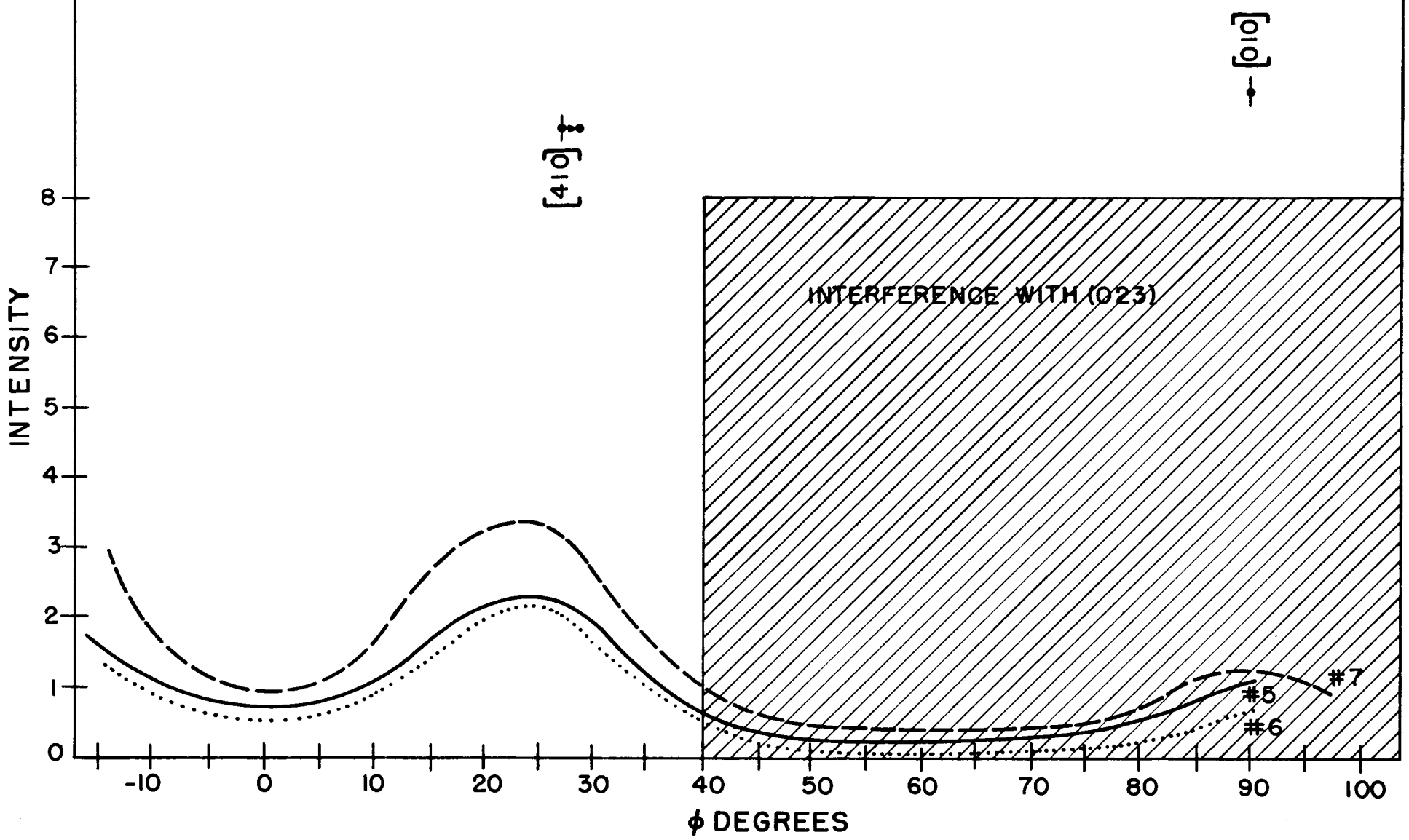

P- 46

DWG. 9764 [redacted]

FIG. 24

PREFERRED ORIENTATION PLOT – (113) – α – EXTRUDED URANIUM

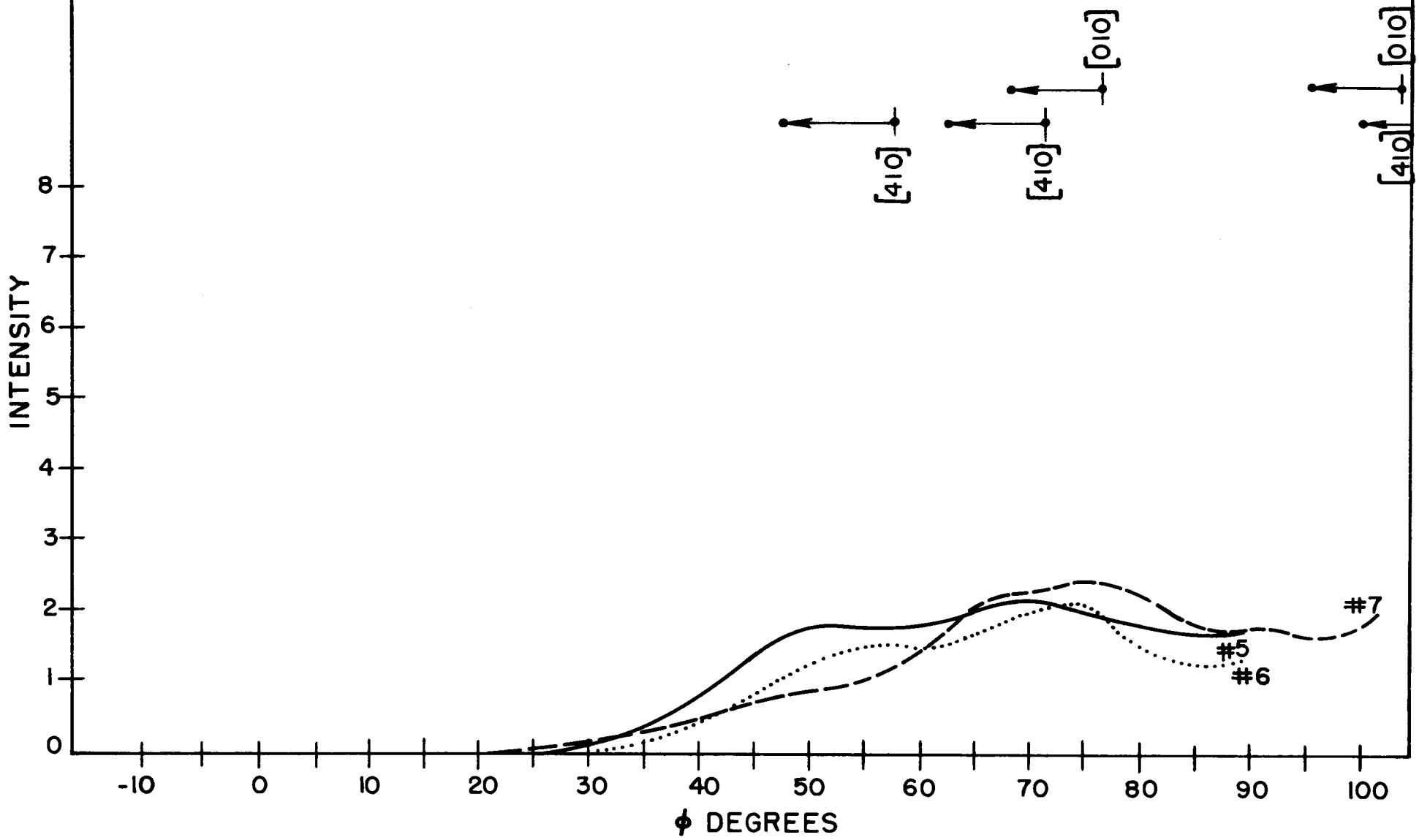

however, are not so comparable because of change in geometry with variation in 2θ value for diffraction of different planes or with variation in size of specimen.

Study of these data revealed the following salient features concerning the nature of the preferred orientation in this sample: the preferred orientation may be described as a duplex fiber texture, the preferred directions in the grains being either [010] or [410]. Near the axis of the cylindrical bar these crystallographic directions are aligned parallel to the extrusion direction. Off the axis, however, these preferred directions are inclined to the extrusion direction as in the zonal or conical fiber textures described by Schmidt and Wassermann and others. The apex of the cone points toward the front end of the bar. On the graphs of Figs. 14 to 24 are indicated the positions of the intensity maxima to be expected for no inclination of the preferred direction and the directions and amounts of shift in the intensity maxima for an inclination of 10°. The smaller specimen (No. 6) shows a less pronounced shift in an intensity maximum than does the larger specimen (No. 5), indicating that the angle of inclination increases with distance from the bar axis--the values range from 0-10°. In conformity with this, the curves for the off-center specimen (No. 7) show either broader maxima or double peaks resulting from integration over material from different parts of the sample as the specimen is rotated during exposure.

The description given above appears to explain adequately the more conspicuous features of the intensity plots although there are some variations in intensity not so explained. For instance, there is a low maximum in intensity at $\phi = 0$ for [002]. It may be that this is a residuum of the ingot grain structure that underwent only slight deformation as a result of low resolved shear stress on the slip plane, and therefore only slight reorientation.

It may be noted that, where a clear distinction can be made (*i.e.*, there are no complications due to the duplexity of the texture), an intensity maximum related to a given texture occurring near $\phi = 0$ is higher than those related to the same texture but occurring at other values of ϕ. This means that at $\phi = 0$ nearly every grain involved in that texture has a plane in the proper orientation for diffraction, whereas at $\phi > 0$, as a result of the random

distribution of orientations around the preferred direction, only some of the grains involved in that texture have a plane in the proper orientation for diffraction. It is desirable to know whether complete randomness is present, so an attempt is being made to compute just what the intensity variation with ϕ should be in this case. The degree of deviation from this relationship would give an indication of development of preferred directions perpendicular or nearly perpendicular to the extrusion direction.

To obtain an indication of the relative prominence of the two textures in the present case, it appears profitable to compare the relative intensities of the [040] and [110] at $\phi = 0$ with the relative intensities expected for random orientation. The values as calculated by Jacobs and Warren are 8 and 87, respectively. The almost equal intensities observed here suggest that the [010] texture is more prominent than the [410]. As mentioned above, quantitative comparisons, however, can not be made unless correction is made in the intensities for the change in diffracting angle. An attempt is now being made to formulate this correction, since one of the objectives of this study is the development of methods of determining preferred orientation in a completely quantitative manner.

Investigation is continuing on samples taken from the front and back ends of the same extruded bar and on samples from 0.9 in. and 5/8 in. diameter bar extruded in a similar manner. Completion of this and other work involving the effect of other variables of extrusion and thermal treatment should give a comprehensive knowledge of the preferred orientation in uranium extrusions and reveal some pertinent facts concerning the deformation and recrystallization mechanism in uranium.

MECHANICAL PROPERTIES OF METALS

URANIUM CREEP TESTING

An investigation of the creep of uranium is being initiated. Two beam loading creep testing machines have been received from Baldwin Locomotive Works. Four additional machines are to be delivered in September.

A vacuum furnace for use with these machines at 1800°F has been designed and built in the research shops. Completion and testing of this furnace now awaits delivery of nickel sheet for heat reflectors.

HEAT AND LIQUID METAL RESISTANT ALLOY TESTING

This program is designed to help select high temperature reactor materials for the ANP program. One screw operated, spring loaded, automatic recording creep rupture machine has been received from the Baldwin Locomotive Works, and five additional machines are to be shipped in September.

Liquid metal container-grip assemblies, for use in furnaces installed on the creep rupture machines, have been designed, and drawings are ready for the research shops which are to manufacture the assemblies.

Shop orders for installation of all creep equipment, electric wiring and plumbing have been issued.

PURE METALS—DEFORMATION RESEARCH

Work on copper at room temperature has been completed and the data are being worked. A memorandum is being written interpreting the hypothesis described in memorandum CF 50-4-75.[1] It was found that the $(\sigma)_v$ surface can be described over the largest portion of the strain-stress-time diagram by a comparatively simple equation containing six constants:

(1) Andersen, A. G. H., *A Study of Stress-Strain-Time Functions of Metal*, ORNL CF 50-4-75 (Apr. 19, 1950).

$$(\sigma)_v = \left[K_1 + (K_3 - K_1)\ \zeta^{-(0.02/\delta)}\right]\ \delta^m + B\delta^n\ t^{-b},$$

over the greatest portions of the diagram reducing to $K\delta^m + F(t)$, and, when time is disregarded, to $K\delta^m$, the usual stress-strain formula. It has been definitely established that in copper, the "constant" K is variable and that the effect of softening with time can be expressed by a hyperbolic surface in δ and t. From the equation for the $(\sigma)_v$ surface, the rates of hardening (f_δ) and softening (f_t) can be found by differentiation. Expressions for the effect of speed of testing, or rates of deformation (f_v) and changes in rates of deformation (f_a) can be similarly found, but yield somewhat complicated expressions. We are now attempting to find simpler expressions for the rate of change of stress with the four vectors, f_δ, f_t, f_v, f_a, so that the stress at any strain rate may be obtained by the line integral over the strain-time path,

$$\sigma = \int\ (f_\delta d\delta + f_t dt + f_v dv + f_a da).$$

Simple expressions for these four vectors will also allow the rate of deformation in creep to be calculated as

$$v = \frac{f_t + af_v + \dot{a}f_a}{f_\delta}.$$

Work is now progressing on testing of copper at higher temperatures so that temperature coefficients on the parameters, K_1, K_3, B, m, n, and b, may be determined.

It is expected that these parameters in various metals and their temperature coefficients will become of special interest in future basic studies of radiation damage to reactor materials, and also that they will be taken into account in the dislocation theory and other theories of plastic deformation.

AIRCRAFT NUCLEAR PROPULSION—MATERIALS PROGRAM

STATIC CORROSION TESTING

This initial phase of the liquid metals corrosion testing program is designed to find suitable high temperature materials of construction for use in contact with various coolants. Sorting tests on the coolants lithium, bismuth, and lead continued, and are being extended to cover sodium, NaK and sodium hydroxide in the 600 to 1000°C temperature range. A group of the metallic elements were corrosion tested in the liquid circulating fuel-type alloys bismuth-2% uranium and lead-2% uranium. A more extensive study of the corrosion behavior of the stainless steels in molten lithium is in progress.

Stainless Steels in Lithium. Stainless steel alloys were corrosion tested in 1000°C (1832°F) lithium for exposure periods of four and 40 hours. The alloys tested included the chromium steels 405, 430 and 446 as well as the austenitic grades 304, 310, 316, and 347.

Tests were conducted in the usual manner of sealing the test specimen plus a controlled amount of lithium in an evacuated Armco iron capsule, heating to the desired temperature, and holding the test capsule at temperature for the specified time. The test specimen surface to lithium volume ratio varied between 0.5 and 0.7. All tests were run in triplicate.

The four and 40 hour results are tabulated in Table VI. Weight change (mg/cm^2) data are reported as an average of the three specimens tested. Penetration as measured by metallographic examination is reported on the photomicrographs. Analysis of the bath metal after test was made spectrographically.

To aid in understanding the nature and depth of attack and to determine the degree of selective leaching of constituents by the bath metal, metallographic examination of the 40 hour test specimens is in progress.

All specimens were cut diagonally and mounted with protective bars at the exposed surface to reduce edge rounding during polishing. Thickness measurements were taken at the center area to compare with similar measurements made on the specimen prior to testing. Maximum corrosion depth reported on the micrographs refers to penetration measured beyond the exposed surface from one side of the specimen. Six fields were measured to obtain a representative value.

TABLE VI

Corrosion Results of Stainless Steels in 1000°C Lithium

Specimen Size 1 in. × ¾ in. × ¼ in.

STAINLESS STEEL ALLOY	NUMBER SAMPLES TESTED	TEST DURATION (hrs)	AVERAGE WEIGHT CHANGE (mg/cm^2)	BATH ANALYSIS AFTER TEST (ppm)	REMARKS
304	3 3	4 40	-1.39 -5.62	-- Fe 20-90; Ni 90-250; Cr N.D.	Moderate resistance; 40 hour micro shows intercrystalline attack to a depth of two mils and some evidence of a phase transformation near the attacked grain boundary.
310	3 3	4 40	-4.08 -30.75	Fe 20-70; Ni 140-250; Cr N.D. Fe 25-54; Ni 310-450; Cr N.D.	Fair resistance; 40 hour micro shows heavy intercrystalline attack to a depth of one mil.
316	3 3	4 40	-1.56 -6.70	-- Fe 23-71; Ni 91-270; Cr N.D.	-- Moderate resistance; 40 hour micro shows intercrystalline type attack to a depth of four mils and some evidence of a possible phase transformation near attacked grain boundary.
347	3 3	4 40	-1.97 -10.49	-- Fe 25-60; Ni 170-200; Cr & Nb N.D.	-- Moderate resistance; micro shows intercrystalline attack to a depth of three mils
405	3 3	4 40	-1.09 -3.44	-- Fe 73-150; Cr N.D.	Good resistance; micro showed practically no intercrystalline attack.

TABLE VI (Cont'd)

STAINLESS STEEL ALLOY	NUMBER SAMPLES TESTED	TEST DURATION (hrs)	AVERAGE WEIGHT CHANGE (mg/cm^2)	BATH ANALYSIS AFTER TEST (ppm)	REMARKS
430	3 3	4 40	-1.26 -4.13	-- --	Good corrosion resistance; micro showed practically no evidence of intercrystalline attack.
446	3 3	4 40	-3.24 -9.79	-- Fe 50-150; Cr N.D.	-- Moderate resistance; micro showed decarburization and grain growth at exposed surface.

The following photomicrographs were prepared for study:

1. Etched transverse section of the specimen showing surface condition and structure prior to testing.

2. Unetched transverse section of corroded specimen showing condition of metal at the exposed surface. Examination of the specimen prior to etching was considered necessary because etching might destroy films or other corrosion effects at the interface.

3. Transverse section of corroded specimen etched with alkaline potassium ferricyanide to bring out the carbide in the structure.

4. Transverse section of corroded specimen etched with oxalic acid to resolve the grain structure.

Photomicrographs on each of the seven stainless alloys tested are shown in Figs. 25 through 31.

Although this investigation is incomplete, the ferritic iron-chromium alloys appear to be somewhat more resistant to 1000°C lithium than the austenitic type alloys on short exposures, although the available evidence is not yet sufficient to recommend the ferritic alloys as container materials. The austenitic grades 304, 310, 316, and 347 were all attacked intergranularly while the ferritic alloys showed less evidence of this type of attack. The high carbon content alloy 446 showed a decarburized area accompanied by marked grain coarsening to a depth of 30 mils. There is evidence that a part of the structure immediately adjacent to the attacked grain boundaries in the 304, 316 and 347 grades has undergone a phase change, *i.e.*, upon slow cooling, a rim of ferrite surrounds the austenite grains, presumably by removal of an austenite-former, probably carbon, by diffusion and solution in the lithium. Further metallographic work is underway to study this transformation.

Four hundred hour exposure tests in 1000°C lithium are in progress. Additional tests at lower temperatures are planned to study the corrosion behavior of the stainless alloys above and below the critical range.

Pure Metals in Lithium. During the quarter, 40-hour tests were completed on the metallic elements and selected high temperature alloys in 1000°C (1832°F) lithium. Results indicate, as did the four-hour tests reported last quarter, that iron, zirconium, molybdenum, tungsten, tantalum, and niobium show good resistance to 1000°C lithium. It should be noted, however, that both the zirconium and columbium specimens gained weight due to film formation. Such

NOT CLASSIFIED

PHOTO NO. Y-2525

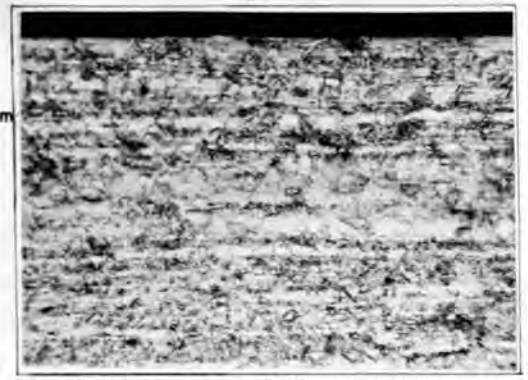

BEFORE EXPOSURE 250X ETCH OXALIC ACID

AFTER EXPOSURE 250X UNETCHED

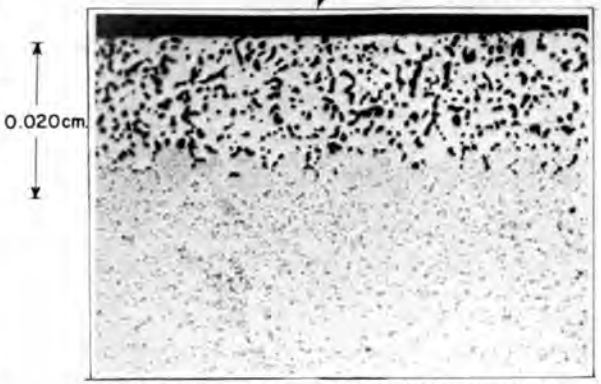

AFTER EXPOSURE 250X ETCH: ALKALINE POTASSIUM FERRICYANIDE

SPECIMEN THICKNESS BEFORE TEST---0.572 cm.
SPECIMEN THICKNESS AFTER TEST---0.569 cm.
MAX. CORROSION DEPTH----------0.018cm.

CENTER OF SPECIMEN

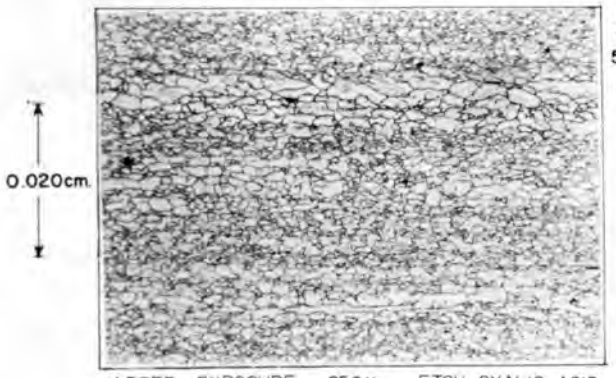

AFTER EXPOSURE 250X ETCH OXALIC ACID

PER CENT COMPOSITION

SPECTROGRAPHIC							VACUUM FUSION			
Fe	Cr	Ni	Mn	Mo	Nb	Al	C	N_2	O_2	H_2
54.4	25.9	19.1	0.15	-	-	-	0.14	0.015	0.012	<0.001

SINGLE SAMPLE

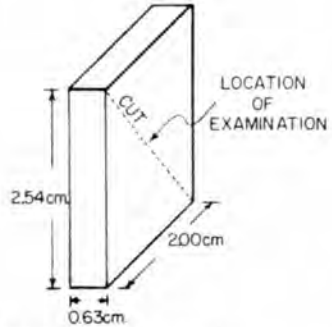

TYPICAL TEST SPECIMEN

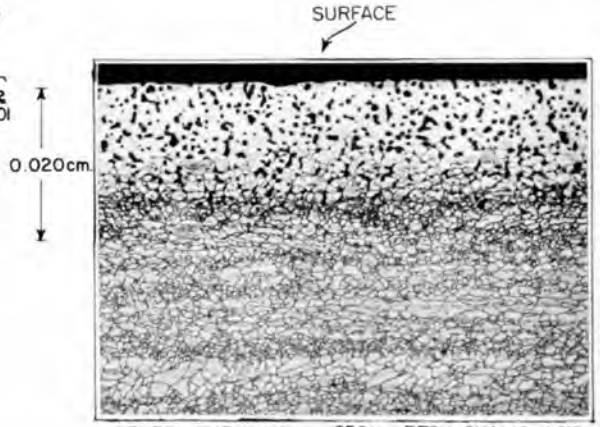

AFTER EXPOSURE 250X ETCH OXALIC ACID

TYPE 310

STAINLESS STEEL EXPOSED TO MOLTEN LITHIUM

R.J. Gray

1000 °C FOR FORTY HOURS

FIG. 25

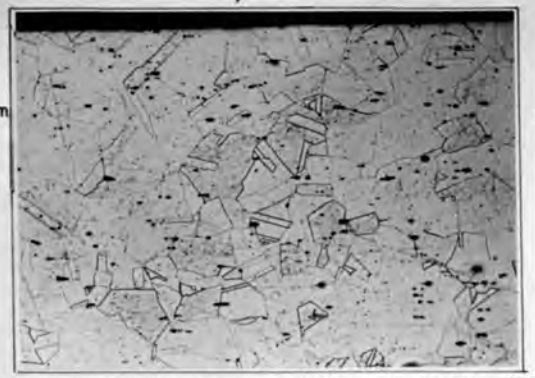

BEFORE EXPOSURE 250X ETCH: GLYCERIA REGIA

AFTER EXPOSURE 250X UNETCHED

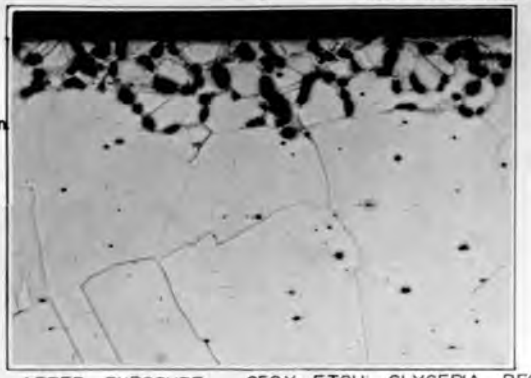

NOT CLASSIFIED
PHOTO NO. Y-2526

AFTER EXPOSURE 250X ETCH: GLYCERIA REGIA

CENTER OF SPECIMEN

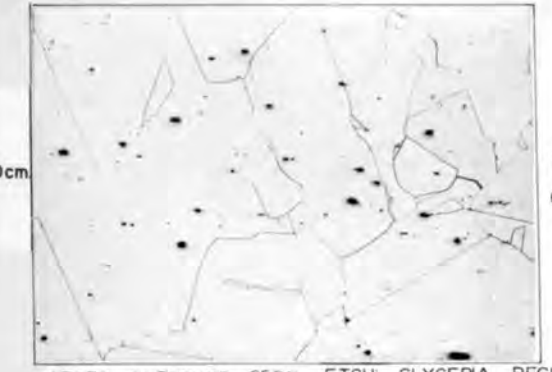

AFTER EXPOSURE 250X ETCH: GLYCERIA REGIA

SPECIMEN THICKNESS BEFORE TEST---0.584 cm.
SPECIMEN THICKNESS AFTER TEST---0.583 cm.
MAX. CORROSION DEPTH------- -0.016 cm.

PER CENT COMPOSITION

SPECTROGRAPHIC								VACUUM FUSION		
Fe	Cr	Ni	Mn	Mo	Nb	Al	C	N_2	O_2	H_2
69.0	16.8	11.7	0.21	2.32	-	-	0.046	0.018	0.015	<0.001

SINGLE SAMPLE

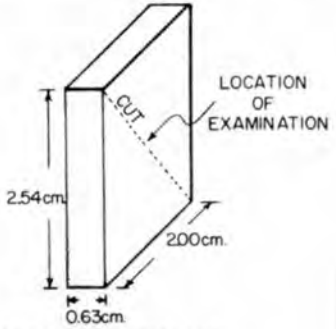

TYPICAL TEST SPECIMEN

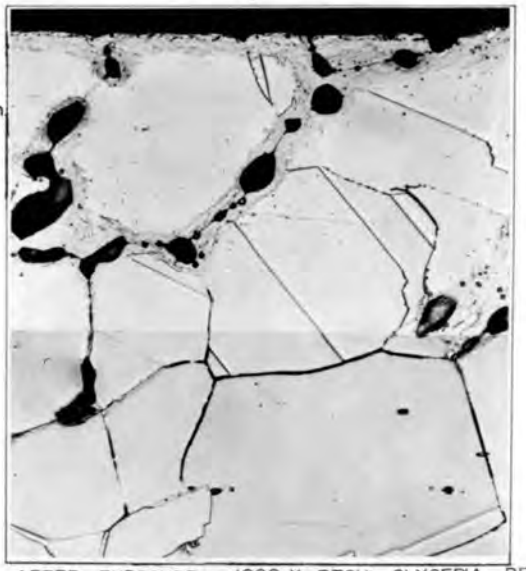

AFTER EXPOSURE 1000 X ETCH: GLYCERIA REGIA

TYPE 316

STAINLESS STEEL EXPOSED TO MOLTEN LITHIUM

1000 °C FOR FORTY HOURS

R.J. Gray

FIG. 26

NOT CLASSIFIED

PHOTO NO. Y-2527

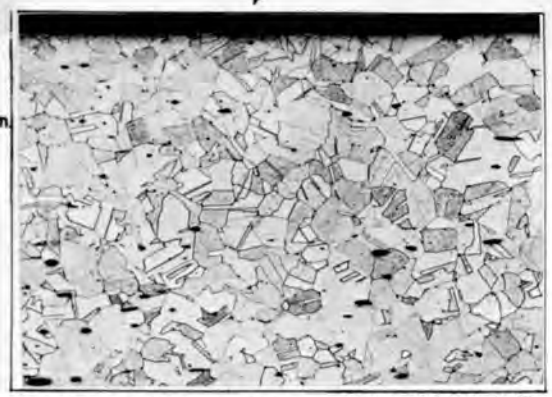

BEFORE EXPOSURE 250X ETCH OXALIC ACID

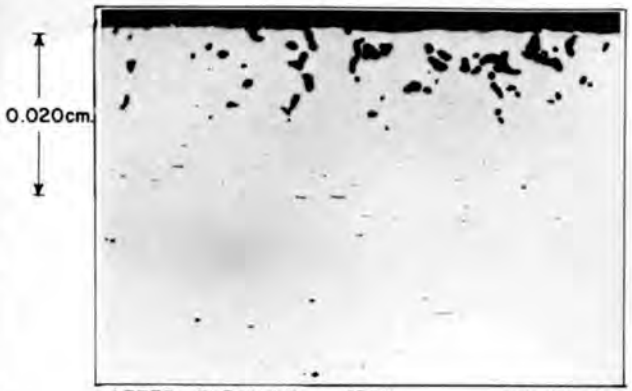

AFTER EXPOSURE 250X UNETCHED

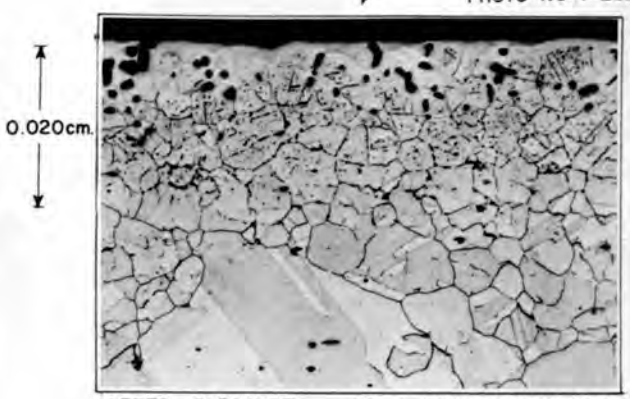

AFTER EXPOSURE 250X ETCH OXALIC ACID

SPECIMEN THICKNESS BEFORE TEST---0.585 cm.
SPECIMEN THICKNESS AFTER TEST---0.584 cm.
MAX. CORROSION DEPTH---------- 0.013 cm.

PER CENT COMPOSITION

SPECTROGRAPHIC								VACUUM FUSION		
Fe	Cr	Ni	Mn	Mo	Nb	Al	C	N_2	O_2	H_2
72.2	17.7	9.76	0.35	-	-	-	0.078	0.019	0.014	<0.001

SINGLE SAMPLE

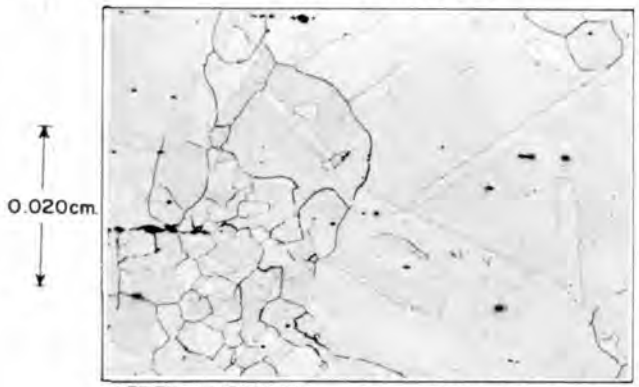

AFTER EXPOSURE 250X ETCH OXALIC ACID

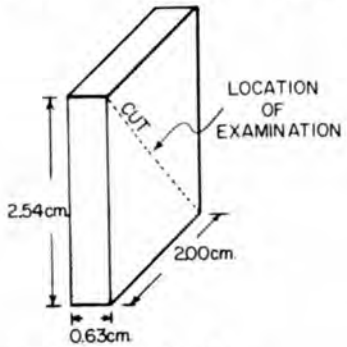

TYPICAL TEST SPECIMEN

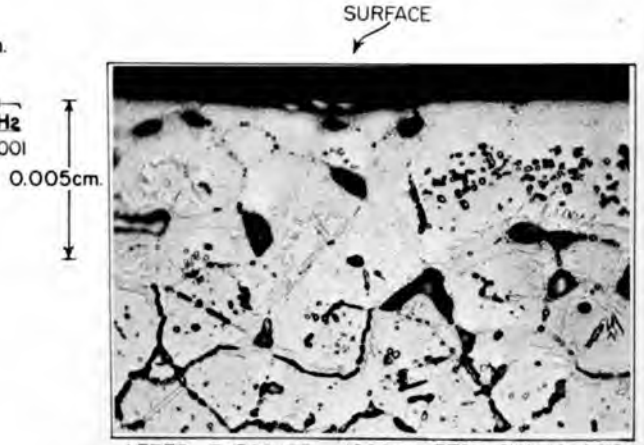

AFTER EXPOSURE 1000 X ETCH OXALIC ACID

TYPE 304

STAINLESS STEEL EXPOSED TO MOLTEN LITHIUM

1000 °C FOR FORTY HOURS

R.J. Gray

FIG. 27

BEFORE EXPOSURE 500X ETCH OXALIC ACID

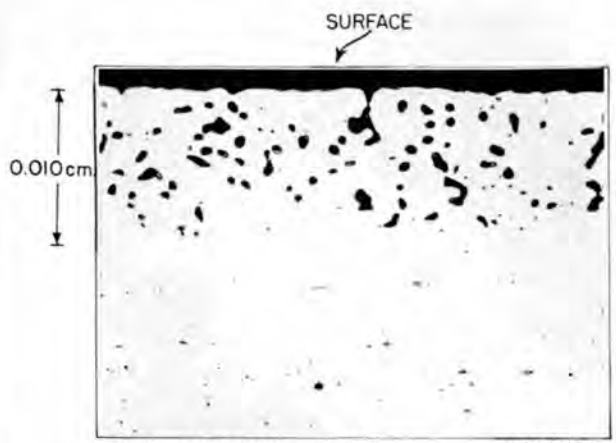

AFTER EXPOSURE 500X UNETCHED

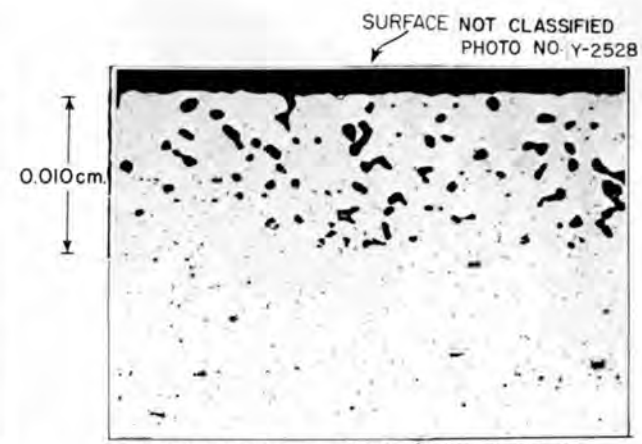

AFTER EXPOSURE 500X ETCH: ALKALINE POTASSIUM FERRICYANIDE

SPECIMEN THICKNESS BEFORE TEST---0.585 cm.
SPECIMEN THICKNESS AFTER TEST---0.584 cm.
MAX. CORROSION DEPTH----------0.011 cm.

CENTER OF SPECIMEN

AFTER EXPOSURE 500X ETCH OXALIC ACID

PER CENT COMPOSITION

SPECTROGRAPHIC								VACUUM FUSION		
Fe	Cr	Ni	Mn	Mo	Nb	Al	C	N_2	O_2	H_2
69.2	19.0	10.2	0.18	-	0.84	-	0.077	0.023	0.003	<0.001

SINGLE SAMPLE

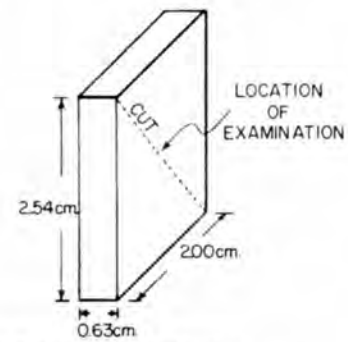

TYPICAL TEST SPECIMEN

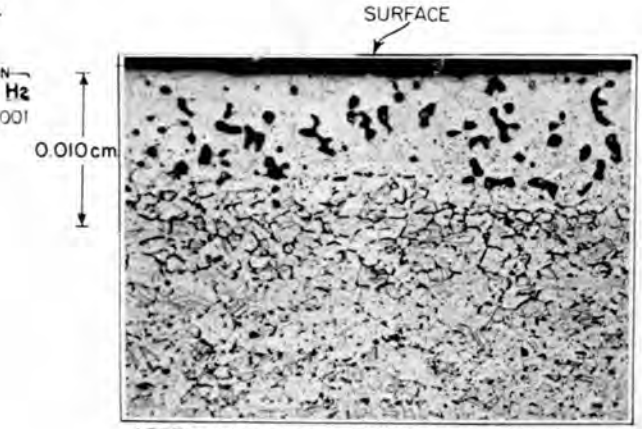

AFTER EXPOSURE 500X ETCH OXALIC ACID

TYPE 347

STAINLESS STEEL EXPOSED TO MOLTEN LITHIUM

1000 °C FOR FORTY HOURS

R.J. Gray

FIG. 28

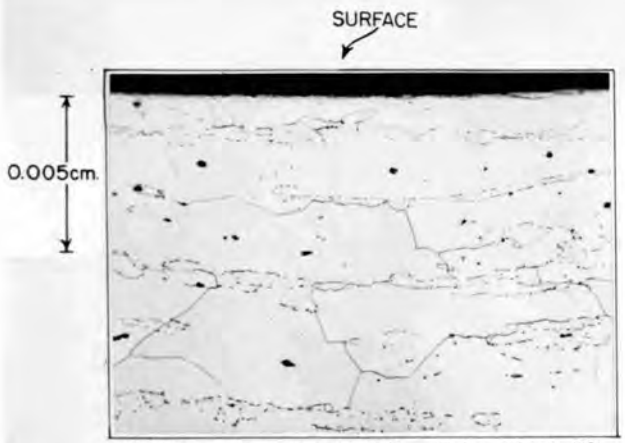

BEFORE EXPOSURE 1000X ETCH: PICRAL-HCL

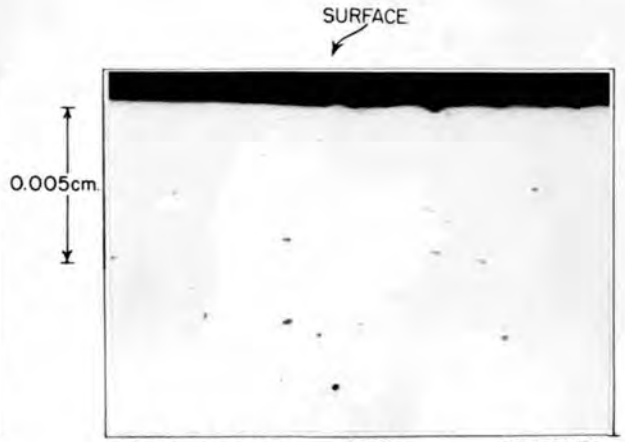

AFTER EXPOSURE 1000X UNETCHED

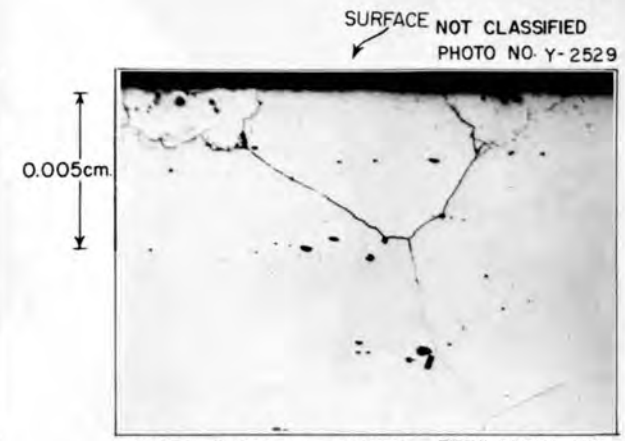

NOT CLASSIFIED
PHOTO NO. Y-2529

AFTER EXPOSURE 1000X ETCH: PICRAL-HCL

SPECIMEN THICKNESS BEFORE TEST---0.587cm.
SPECIMEN THICKNESS AFTER TEST---0.586cm.
PARTIAL SOLUTION----------0.003cm.

PER CENT COMPOSITION

SPECTROGRAPHIC								VACUUM FUSION		
Fe	Cr	Ni	Mn	Mo	Nb	Al	C	N_2	O_2	H_2
86.3	13.3	-	-	-	-	0.42	0.078	0.018	0.003	<0.001

SINGLE SAMPLE

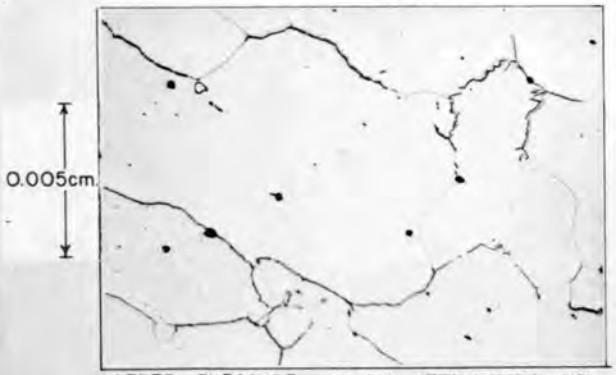

AFTER EXPOSURE 1000X ETCH: PICRAL-HCL

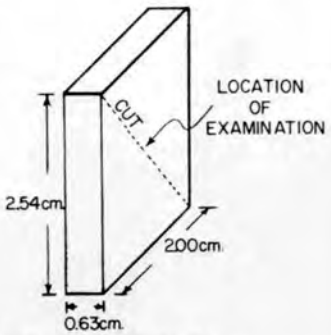

TYPICAL TEST SPECIMEN

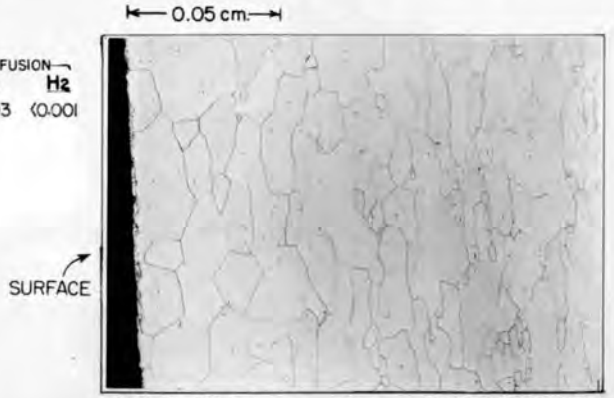

AFTER EXPOSURE 100X ETCH: PICRAL-HCL

TYPE 405

STAINLESS STEEL EXPOSED TO MOLTEN LITHIUM

1000 °C FOR FORTY HOURS

FIG. 29

R.J. Gray

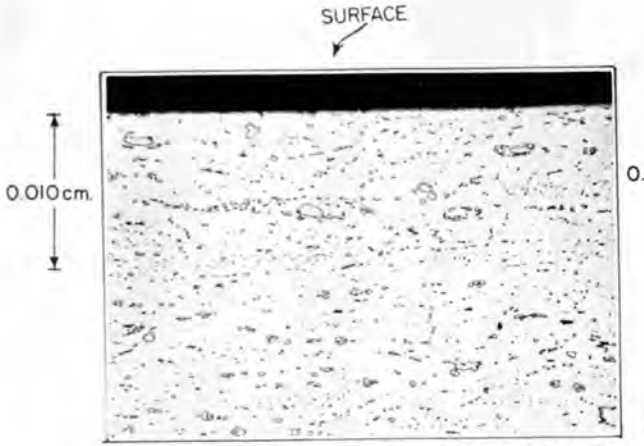

BEFORE EXPOSURE 500X ETCH: PICRAL-HCL

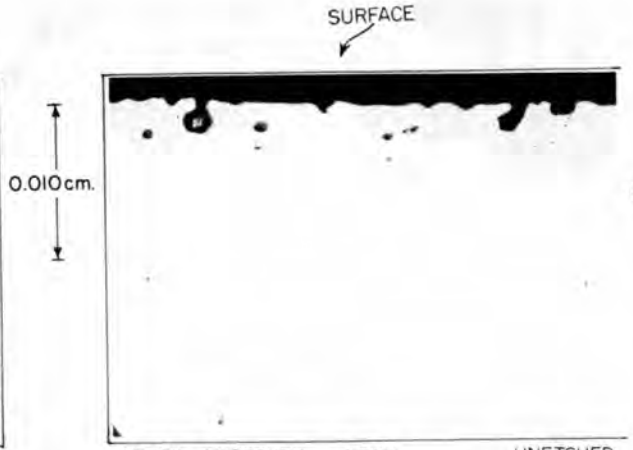

AFTER EXPOSURE 500X UNETCHED

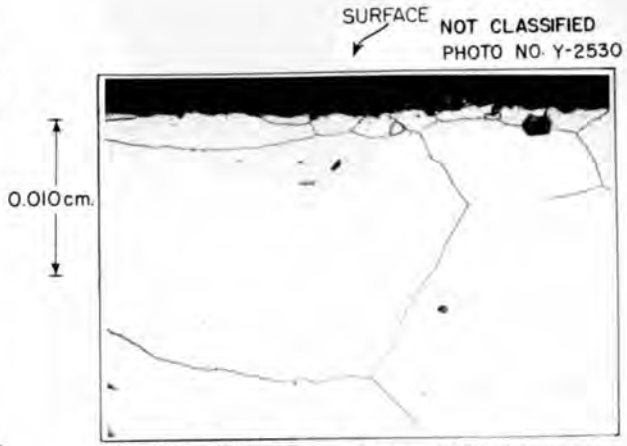

AFTER EXPOSURE 500X ETCH: PICRAL-HCL

SPECIMEN THICKNESS BEFORE TEST-----0.631 cm.
SPECIMEN THICKNESS AFTER TEST-----0.627 cm.
PARTIAL SOLUTION----------0.015 cm.

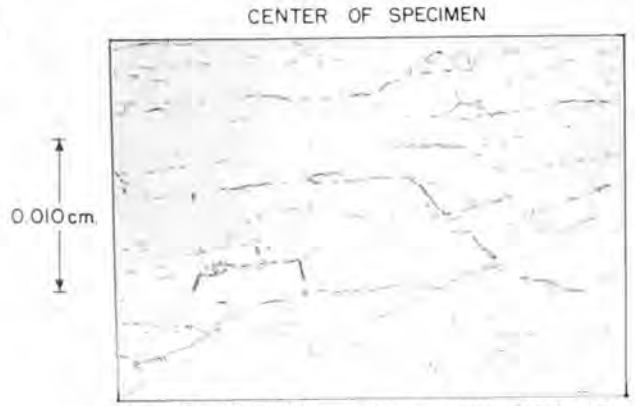

AFTER EXPOSURE 500X ETCH: PICRAL-HCL

PER CENT COMPOSITION

SPECTROGRAPHIC							VACUUM FUSION			
Fe	Cr	Ni	Mn	Mo	Nb	Al	C	N_2	O_2	H_2
73.5	25.5	-	-	-	-	-	0.084	0.046	0.009	<0.001

SINGLE SAMPLE

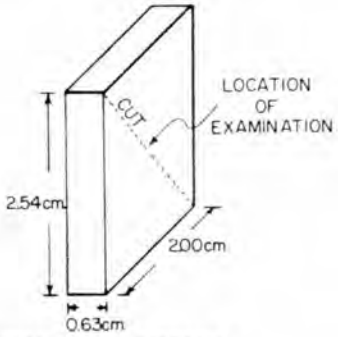

TYPICAL TEST SPECIMEN

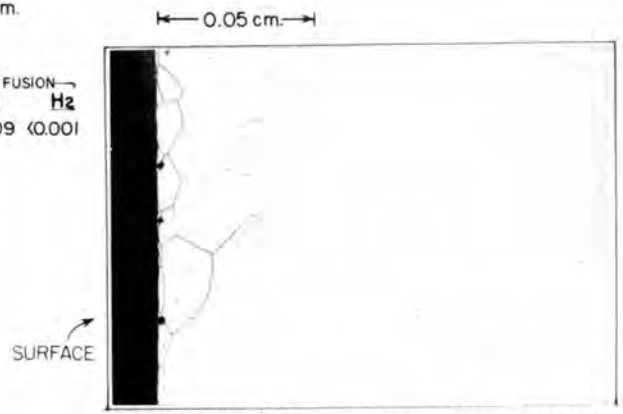

AFTER EXPOSURE 100X ETCH: PICRAL-HCL

TYPE 446

STAINLESS STEEL EXPOSED TO MOLTEN LITHIUM

1000 °C FOR FORTY HOURS

R.J. Gray

FIG. 30

BEFORE EXPOSURE 1000 X ETCH PICRAL-HCL

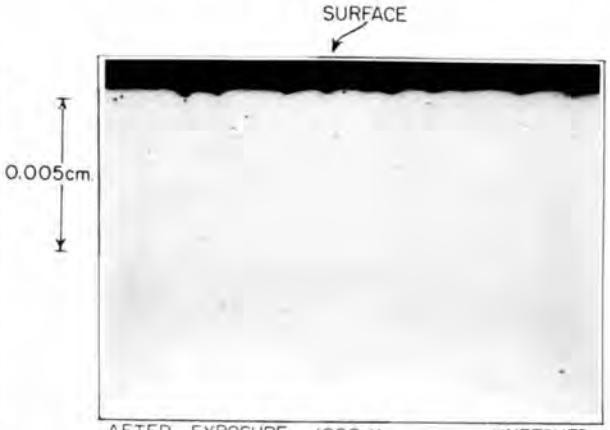

AFTER EXPOSURE 1000 X UNETCHED

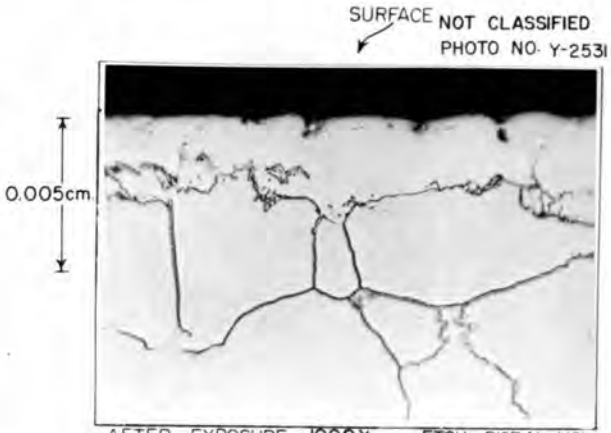

AFTER EXPOSURE 1000X ETCH. PICRAL-HCL

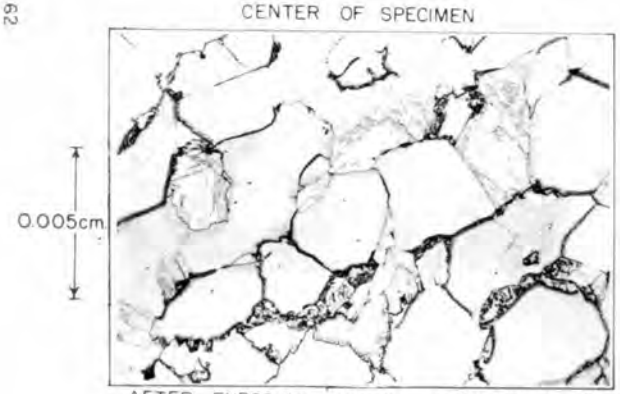

AFTER EXPOSURE 1000X ETCH. PICRAL-HCL

SPECIMEN THICKNESS BEFORE TEST---0.577cm.
SPECIMEN THICKNESS AFTER TEST---0.575cm.
PARTIAL SOLUTION --------0.008cm.

PER CENT COMPOSITION

SPECTROGRAPHIC							VACUUM FUSION			
Fe	Cr	Ni	Mn	Mo	Nb	Al	C	N_2	O_2	H_2
85.0	14.9	-	-	-	-	-	0.080	0.020	0.006	<0.001

SINGLE SAMPLE

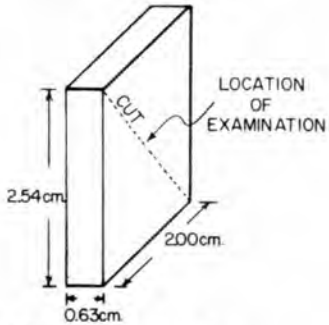

TYPICAL TEST SPECIMEN

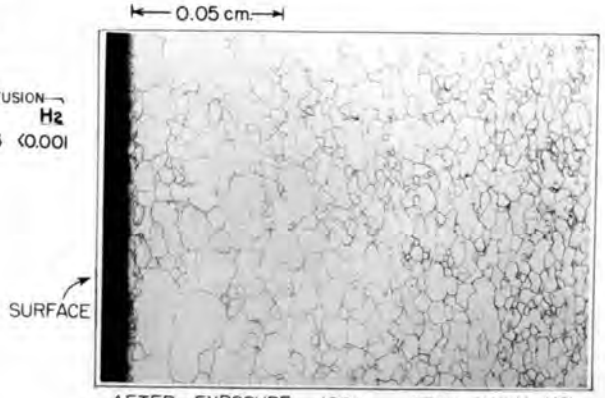

AFTER EXPOSURE 100X ETCH. PICRAL-HCL

TYPE 430

STAINLESS STEEL EXPOSED TO MOLTEN LITHIUM

1000 °C FOR FORTY HOURS

R.J. Gray

FIG. 31

films might be acting as protective coatings which prevent further corrosion. A single test shows practically no attack of uranium by lithium at 1000°C.

In the case of tungsten, molybdenum, and cobalt, mass-transfer of the metal from the specimen to the iron capsule was noted. Removal of the iron from the test system should prevent this transfer and improve the apparent corrosion behavior of these elements. A similar but more striking mass-transfer of metal was observed in the four-hour silicon test in 1000°C (1832°F) lithium.

The 40-hour test results are tabulated along with the four-hour results in Table VII. Four hundred-hour tests are now in progress.

Refractories in Lithium. BeO and several other commercial refractories that might find possible application in reactor construction were corrosion tested in 1000°C lithium. Four-hour exposure tests were run on beryllium oxide, aluminum oxide, chromite, cordierite, silicon carbide, quartz, boron carbide, alundum, zirconium oxide, magnesium oxide, clay-graphite, and graphite. As expected, all disintegrated except the beryllium oxide which showed a moderate weight loss. A similar 100-hour exposure test showed the hot-pressed beryllium oxide grade to be more resistant to 1000°C lithium than the refractory grade.

Pure Metals in PbU and BiU. Because of interest in the dissolved circulating fuel type reactor, exploratory corrosion tests were conducted to find potential materials for containing uranium-bearing metallic solvents. The lead-uranium and bismuth-uranium binary systems look most promising from a uranium solubility viewpoint and for this reason were selected for these tests. The literature shows lead will dissolve up to 0.52 atomic percent uranium at 900°C (1652°F) while upwards of 25% uranium is soluble in liquid bismuth at 1000°C (1832°F). The minimum solubility of uranium in the coolant thought necessary for successful reactor operation is the order of one atomic percent.

The materials tested were confined to some of the high melting metallic elements.

Tungsten	Titanium	Tantalum
Iron	Molybdenum	Nickel
Columbium	Beryllium	Zirconium

TABLE VII

Corrosion Data on the Pure Metals in 1000°C Lithium

Specimen Size 1 in. × ¾ in. × ¼ in. Surface-Volume Ratio 0.6-1.0

METAL	NUMBER SAMPLES TESTED	TEST DURATION (hrs)	AVERAGE WEIGHT CHANGE (mg/cm2)	EQUIVALENT PENETRATION, BASED ON WEIGHT CHANGE (mils)	BATH ANALYSIS AFTER TEST (ppm)	REMARKS
Extruded Beryllium	3 3	4 40	-17.19 -67.82	-3.68 -14.67	-- Fe 140-930; Be 530-9600	Severely attacked; micro shows non-continuous film and large voids. X ray identified only Be
Silicon	3	4	Completely lost	--	--	All three samples apparently dissolved and deposited on capsule wall.
Titanium	3 3	4 40	+ 3.81 - 1.46	+0.33 -0.13	-- Fe 40-310; Ti 43-760	Continuous adherent film formed identified by X ray as TiN.
Vanadium	1	4	- 7.68	-0.50	Fe 37,000 V N.D.	Continuous non-uniform film formed. X ray showed VN, V_2N, V, and Fe_α.
Chromium	1	4	- 5.72	-0.31	Fe 8200; CR N.D.	X ray showed only Cr.
Manganese	3	4	--	--	--	Only thin electrolytic strip tested which apparently dissolved.
Armco Iron	3 3	4 40	- 0.12 - 0.95	-0.01 -0.05	-- Fe 53-1100	-- Good resistance; micro shows no noticeable attack.
Sintered Cobalt	2 3	4 40	- 5.00 -23.35	-0.22 -1.03	-- Fe 210-31,000; Co 150-3100	Non-uniform etching attack. X ray showed α Fe.
"A" Nickel	3	4	-86.41	-3.82	--	Severe intercrystalline type attack; X ray showed only Ni.

N.D. Analysis for but not detected.

TABLE VII (Cont'd)

METAL	NUMBER SAMPLES TESTED	TEST DURATION (hrs)	AVERAGE WEIGHT CHANGE (mg/cm^2)	EQUIVALENT PENETRATION, BASED ON WEIGHT CHANGE (mils)	BATH ANALYSIS AFTER TEST (ppm)	REMARKS
Bureau Mines Zirconium	5 4	4 40	+0.25 +1.09	+0.02 +0.07	-- Fe 72-1300; Zr ND-32	Good resistance; all samples developed brassy tarnish identified by X ray as ZrN.
Sintered Columbium	3 2	4 40	-0.84 +1.06	-0.04 +0.05	-- Fe 2, 600, Cb N.D.	Good resistance; micro showed continuous film not yet identified.
Sintered Molybdenum	3 3	4 40	+0.23 -18.02	+0.01 -0.69	-- Fe 91-1000; Mo N.D.	Good resistance on short term exposure; longer exposure showed Mo deposited on Fe capsule wall.
Sintered Tantalum	3 3	4 40	-1.29 -2.90	-0.04 -0.07	-- Fe ND-1900, 3300-8700 Ta	Good resistance; four hour specimen showed continuous thin film identified as TaC.
Sintered Tungsten	3 3	4 40	-2.63 -32.69	-0.05 -0.67	Fe 900-1300, W-N.D.	Excellent resistance on short exposure; tungsten deposited on capsule wall on longer exposure.
Uranium	1	4	--	--	--	--
1040 Steel	3	4	-2.08	-0.10	--	Micro showed decarburization throughout entire ¼ in. specimen.
Haynes Metamic LT-1	3	4	-120.81	-3.11	--	Drastic attack; all samples exfoliated.
Haynes Alloy L605	3	4	-6.78	-0.29	--	Micro showed areas leached out immediately below exposed surface.
Allegheny Alloy V-36	3	40	-44.02	-1.89	Ni 680-1100, Fe 470-1000, Nb 260-1400, Cr 59-270	Poor resistance.

Corrosion specimens 1 in. × ¼ in. × 3 in. were prepared from strip stock and were immersed in the uranium bearing coolant by means of a vertical positioning rod. See sectional view of test apparatus in Fig. 32. The BeO crucible containing the coolant was housed in a cylindrical quartz tube heated externally by an electric resistance-type furnace. Tube ends were sealed with metal and rubber gasket fittings to permit conventional evacuation and purging of the test chamber prior to operation under an inert atmosphere.

The bismuth and lead bath metals contained approximately two atomic percent uranium for all tests; however, this amount may be in excess of the solubility of uranium in lead. Test temperature was 1000°C (1832°F) and initial test duration was four hours at temperature.

Preliminary results showed substantial attack on most metals tested, with formation of films in most cases.

Beryllium in lead-uranium formed a coating identified as UBe_9 by X-ray examination. The refractory metals—molybdenum, tantalum, tungsten, and columbium—appeared most suited for containing the lead-uranium and bismuth-uranium alloys. Specimens before and after test are shown in Figs. 33 and 34.

Longer time (100 hrs) tests on these metals indicated molybdenum and columbium were still resistant, while tantalum gained excessive weight. Molybdenum showed excellent resistance to lead-uranium alloy on the 100-hr exposure.

Pure Metals in Lead. Preliminary screening tests on some of the metallic elements indicated moderately good resistance of tungsten, zirconium, iron, and tantalum; fair resistance of molybdenum, columbium and beryllium; and poor resistance of titanium and nickel, to lead at 1000°C (1832°F) for 40-hour exposure. Detailed results will be reported upon completion of X-ray and metallographic examination of the test specimens now in progress.

Materials in Sodium Hydroxide. Several pure metals, stainless steel alloys, and refractories were corrosion tested in 1000°C (1832°F) sodium hydroxide with the hope of finding potential materials for use in reactor core construction. Forty-hour tests were run in the usual manner, with nickel substituted for Armco iron as the capsule container. With the possible exception of the container nickel, all the metallic materials tested were drastically attacked. Caustic attack on the stainless alloys was characterized by an exfoliation type attack.

NOT CLASSIFIED
DWG. 9082
Fig. 32

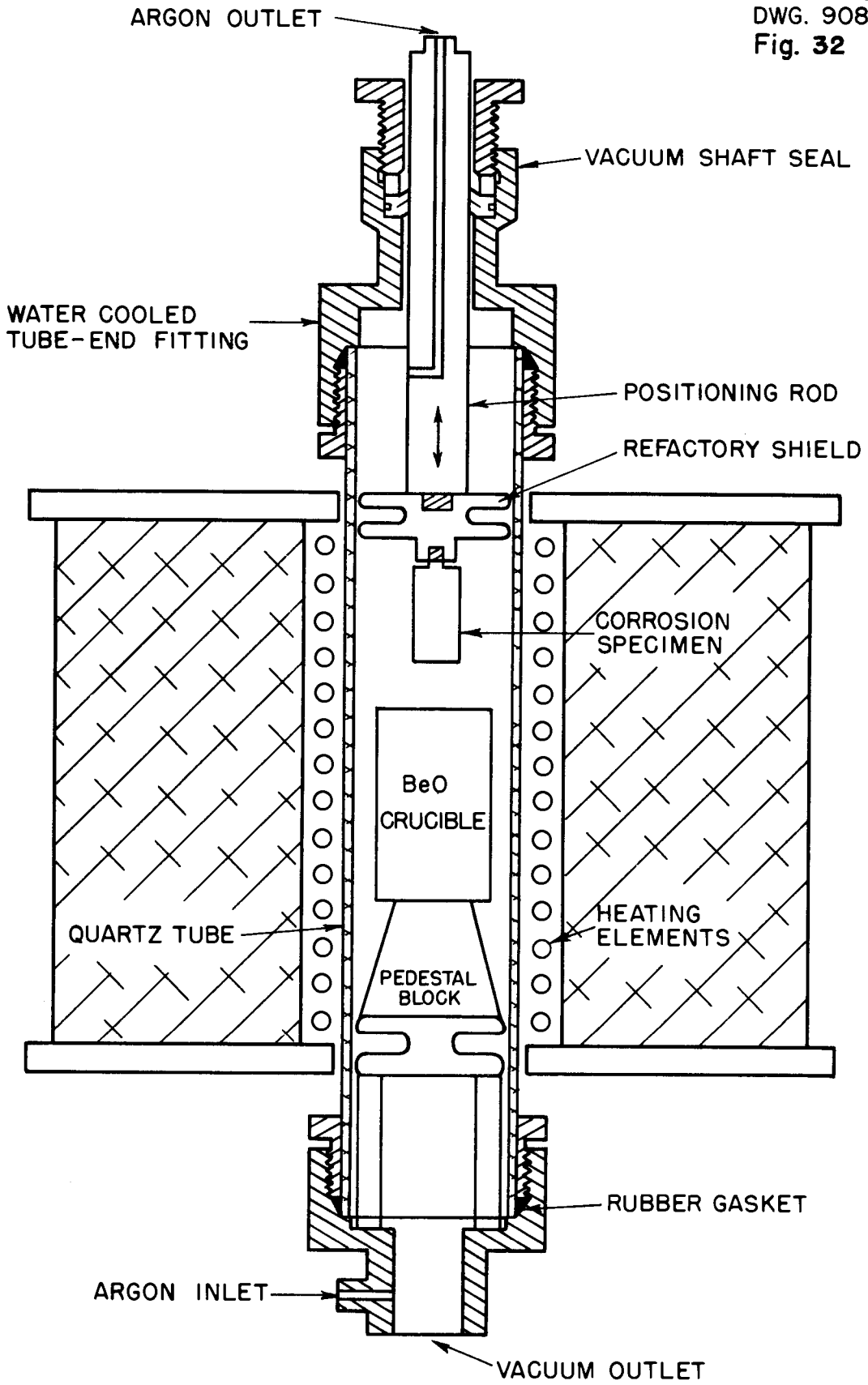

SECTIONAL VIEW VACUUM ARGON CORROSION TESTING APPARATUS

CORROSION IN LIQUID Pb-U & Bi-U ALLOYS

PHOTO NO. Y-2
NOT CLASSIFIED

SPECIMENS BEFORE TEST

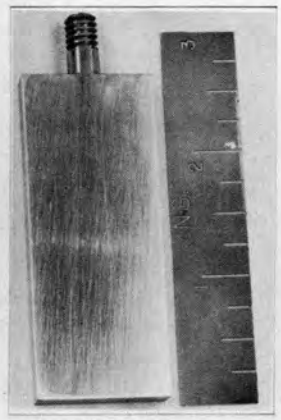

MOLYBDENUM

TANTALUM

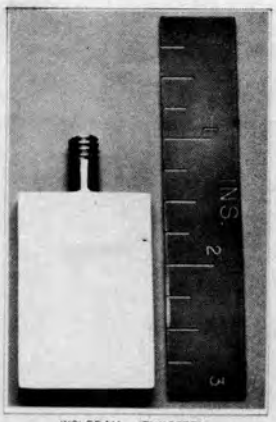

WOLFRAM (TUNGSTEN)

THORIUM

SPECIMENS AFTER FOUR HOURS EXPOSURE IN Pb-U ALLOY (2 at.% U) AT 1000°C

MOLYBDENUM

TANTALUM

WOLFRAM (TUNGSTEN)

THORIUM

SPECIMENS AFTER FOUR HOURS EXPOSURE IN Bi-U ALLOY (2 at.% U) AT 1000°C

MOLYBDENUM

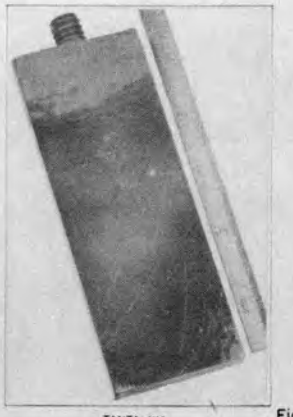

TANTALUM

WOLFRAM (TUNGSTEN)

NO TEST

THORIUM

Fig. 33

CORROSION IN LIQUID Pb-U & Bi-U ALLOYS

PHOTO NO. Y-2533
NOT CLASSIFIED

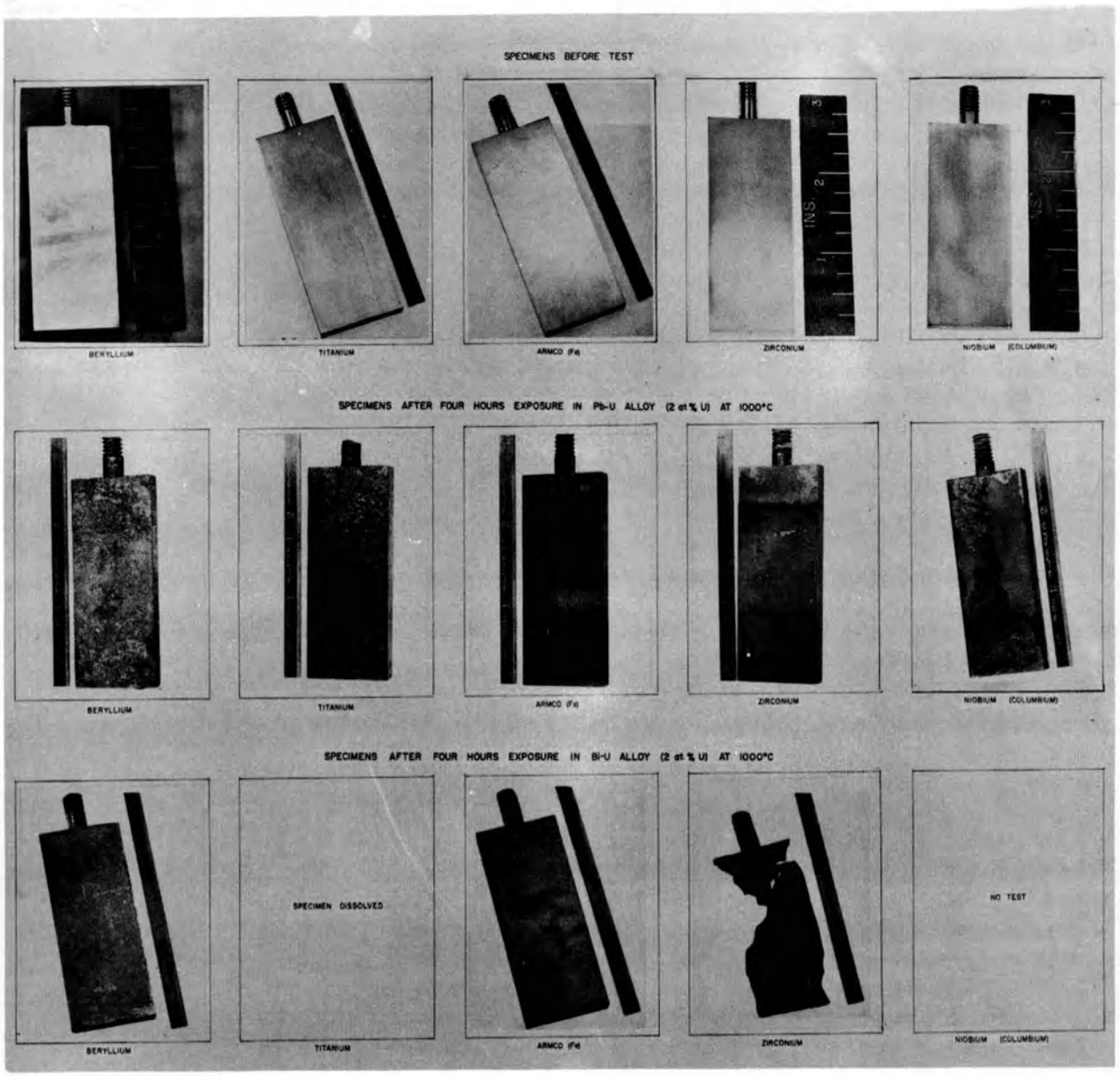

Fig. 34

E. P. GRIGGS

The high fired grade of BeO appeared most resistant of the materials tested. Graphite showed moderate resistance on this short exposure.

In spite of the precautions exercised in canning, numerous capsule leaks were encountered during the heating cycle. These leaks are believed to be a result of excessive internal pressure developed during decomposition of the contaminants sodium carbonate and water. The combined amount of water and sodium carbonate present in the commercial grade of hydroxide is approximately 1% by weight.

CIRCULATING CORROSION TESTING

Thermal Convection Loops (Harps). The following harps have been fabricated:

MATERIAL	NO. OF HARPS	FABRICATOR
Low carbon iron	2	ORNL Shops
Type 304 stainless steel	4	ORNL Shops
Type 310 stainless steel	2	Philadelphia Pipe Bending Co.
Type 347 stainless steel	4	ORNL Shops
Alloy L605	1	Philadelphia Pipe Bending Co.
Nickel	4	ORNL Shops

V 36 alloy tubing has been supplied to Philadelphia Pipe Bending Company for fabrication in the latter part of July.

Shrouded, or clad tubing with a low carbon steel core has been completed and is awaiting clad sheet stock for harp fabrication at Philadelphia Pipe Bending Company.

Titanium tubing and plate have been furnished by Allegheny Ludlum to Superior Tube Company for fabrication. Allegheny Ludlum and its affiliate, Titanium Metal Corporation of America, will advise on the fabrication of this material.

Molybdenum tubing will be supplied by Fansteel, and they would like to undertake harp fabrication provided they have progressed sufficiently in their welding and other joining techniques to take on such a fabrication problem.

Other fabrication sources are being investigated. Westinghouse Electric Research Laboratories at East Pittsburgh and Wright Field are considering the problem.

Tantalum tubing can be obtained. Fansteel will undertake the fabrication of a tantalum harp upon the receipt of our purchase order. Because of the possible lack of future interest in tantalum, the order has not yet been placed.

Stainless steels, Types 446 and 316, will be fabricated into harps by the Philadelphia Pipe Bending Company.

Inconel tubing and sheet will be procured for harp fabrication by Philadelphia Pipe Bending Company.

Tanks for housing the harps in an inert atmosphere during testing, are scheduled for August delivery. An initial group of three will be constructed and tried before additional tanks are ordered and equipped. Auxiliary parts, filling and evacuation connections, thermocouple panels, electric supply line connections, etc., are being made up. Pumping and gas purification systems are being specified.

The lithium and sodium melting and purification tanks are being constructed in the research shops.

The harps will in general be operated by the ANP Experimental Engineering Group, with metallurgical control and examination to be done by the ANP Materials Group in the Metallurgy Division.

ANP FUEL ELEMENT FABRICATION PROGRAM

Powder Metallurgy. Equipment is being obtained to equip a small but versatile powder metallurgy laboratory for use in the experimental development of fuel elements and reactor components. Two presses one of 20 tons and the other of 60 to 80 tons capacity will be available for either hot or cold pressing. A variety of sintering equipment providing either inert atmosphere or vacuum sintering is being ordered. A complete set of crushing, grinding, sizing and powder preparation equipment will be installed.

FUNDAMENTAL RADIATION EFFECTS INVESTIGATION

EFFECT OF NEUTRON IRRADIATION ON COPPER ALLOYS

Copper-Beryllium. Previous experimental solution-quenched Cu-Be alloys[1] indicate that radiation damage effects—as measured by change of electrical resistance—saturate with relatively small irradiation exposures. During the past quarter the electrical resistance of an alloy containing 2% Be was measured during irradiation in the Oak Ridge reactor. These measurements were made daily for a period of eight weeks, at the end of which they had to be discontinued because of the failure of the bakelite holder. The resistance was still increasing at a slow rate after eight weeks of irradiation. A plot of percent change of resistance with exposure is shown in Fig. 35.

Other specimens of this alloy were irradiated for periods of three weeks and six weeks. Electrical resistance and hardness measurements were made before and after irradiation. The changes in resistance and hardness due to irradiation for these specimens were:

EXPOSURE	INCREASE IN ELECTRICAL RESISTANCE	INCREASE IN HARDNESS
6 weeks—3.31×10^{18} nvt	11.1%	46.8 DPH
3 weeks—1.67×10^{18} nvt	9.6%	38.3 DPH

These specimens were then aged at various temperatures simultaneously with non-irradiated specimens in order to determine whether the rate of precipitation of the gamma phase was affected by irradiation. Electrical resistance measurements at various aging times indicated that a difference in rate of precipitation did exist. An effort was made to verify this by metallographic investigation, the results of which were inconclusive. A single crystal of this alloy has been prepared and will be used to study the effect of prior irradiation on the precipitation reaction by examining the Guinier-Preston zone streaks on a Laue photograph.

(1) Siegel, S. and Billington, D., "Effect of Reactor Radiation on Metals," *Journal of Metallurgy and Ceramics*, No. 2, TID 66, 54 (Jan., 1949).

DWG. 9765
Not Classified

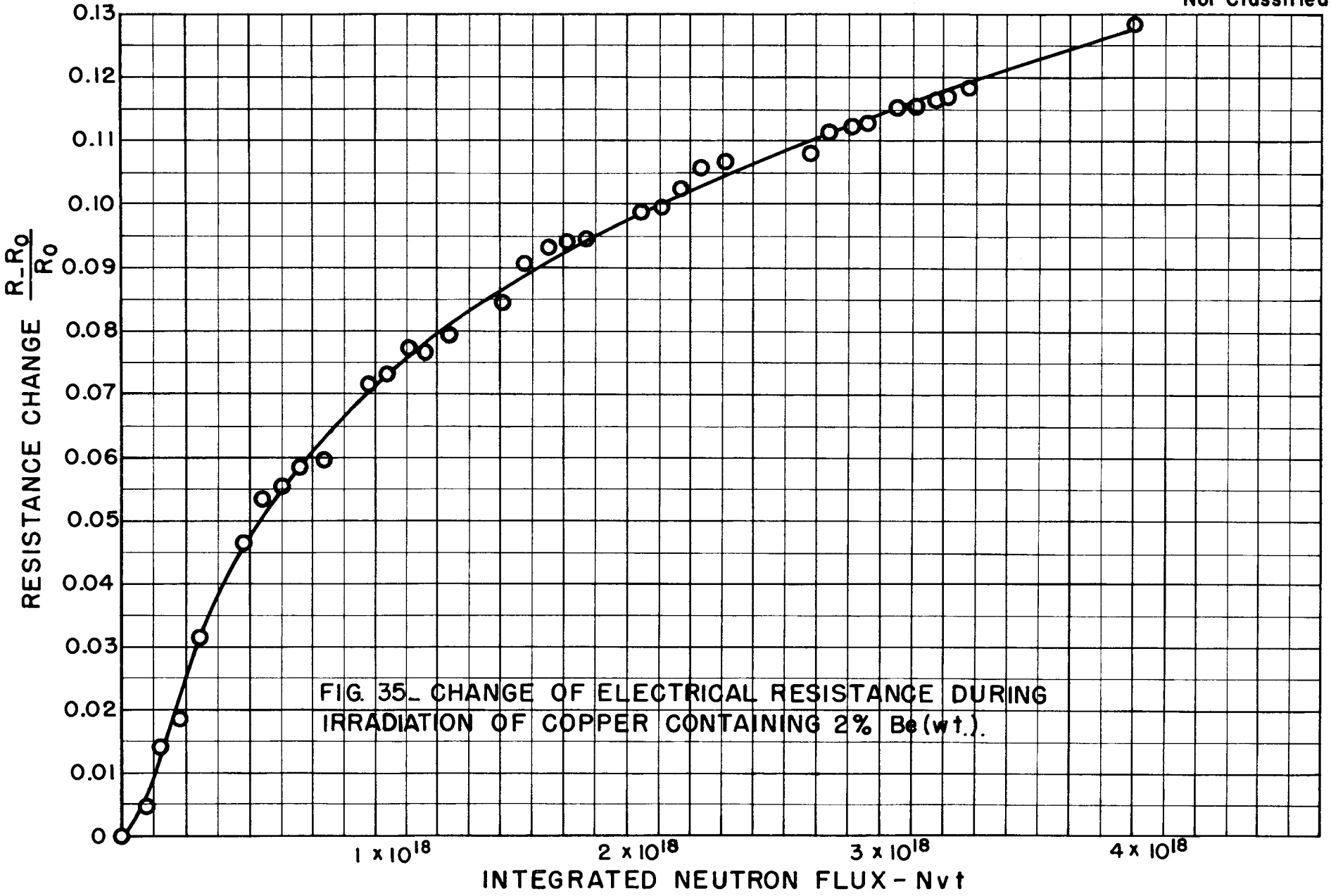

FIG. 35_ CHANGE OF ELECTRICAL RESISTANCE DURING IRRADIATION OF COPPER CONTAINING 2% Be (wt.).

X-ray investigation revealed a marked broadening of the lines in the back-reflection region and an apparent decrease in intensity with increasing θ after irradiating the copper-beryllium alloy. This is the same effect which is observed upon cold working. The lines were sufficiently broadened and weakened to preclude parameter measurement.

Cu-Sn alloys containing 1.8% and 5% Sn by weight were irradiated for a period of three weeks in the ORNL reactor. The measured electrical resistance and hardness changes were:

ALLOY (%)	EXPOSURE (nvt)	INCREASE IN ELECTRICAL RESISTANCE (%)	INCREASE IN HARDNESS (DPH)
1.8 Sn	1.70×10^{18}	0.39	24.2
5 Sn	1.70×10^{18}	0.27	17.0

The fact that the increase in resistance of the 1.8% Sn alloy is higher than the 5% Sn is insignificant since the accuracy of the measurements was only ± 0.15%. Specimens of Cu-Sn alloy, containing 10% Sn by weight, and various compositions of Cu-Mn alloys, are being irradiated.

Copper-Aluminum. The investigation of electrical resistance changes in solid solution alloys of aluminum in copper has been continued. The decrease in resistance during irradiation which occurred in this series and in certain copper-zinc samples is opposite in direction to that observed in other alloy systems and is reported in ORNL 576.[2] During the present period experiments were carried out in an attempt to understand this behavior in copper-aluminum alloys.

Three irradiated samples containing 9.5 atomic percent aluminum were isothermally annealed at different temperatures, together with three unirradiated blanks. Resistance changes during annealing were followed as a function of time. The experimental results are shown in Fig. 36 where the fractional changes in resistance during the anneal is plotted against the logarithm of annealing time. The resistance before irradiation was taken as R_0.

(2) Billington, D. S. and Kernohan, R. H., "Effect of Radiation on Metals," *Physics Division Quarterly Progress Report for Period Ending December 15, 1949*, ORNL-576, 5 (Feb. 7, 1950).

NOT CLASSIFIED

DWG. 9766

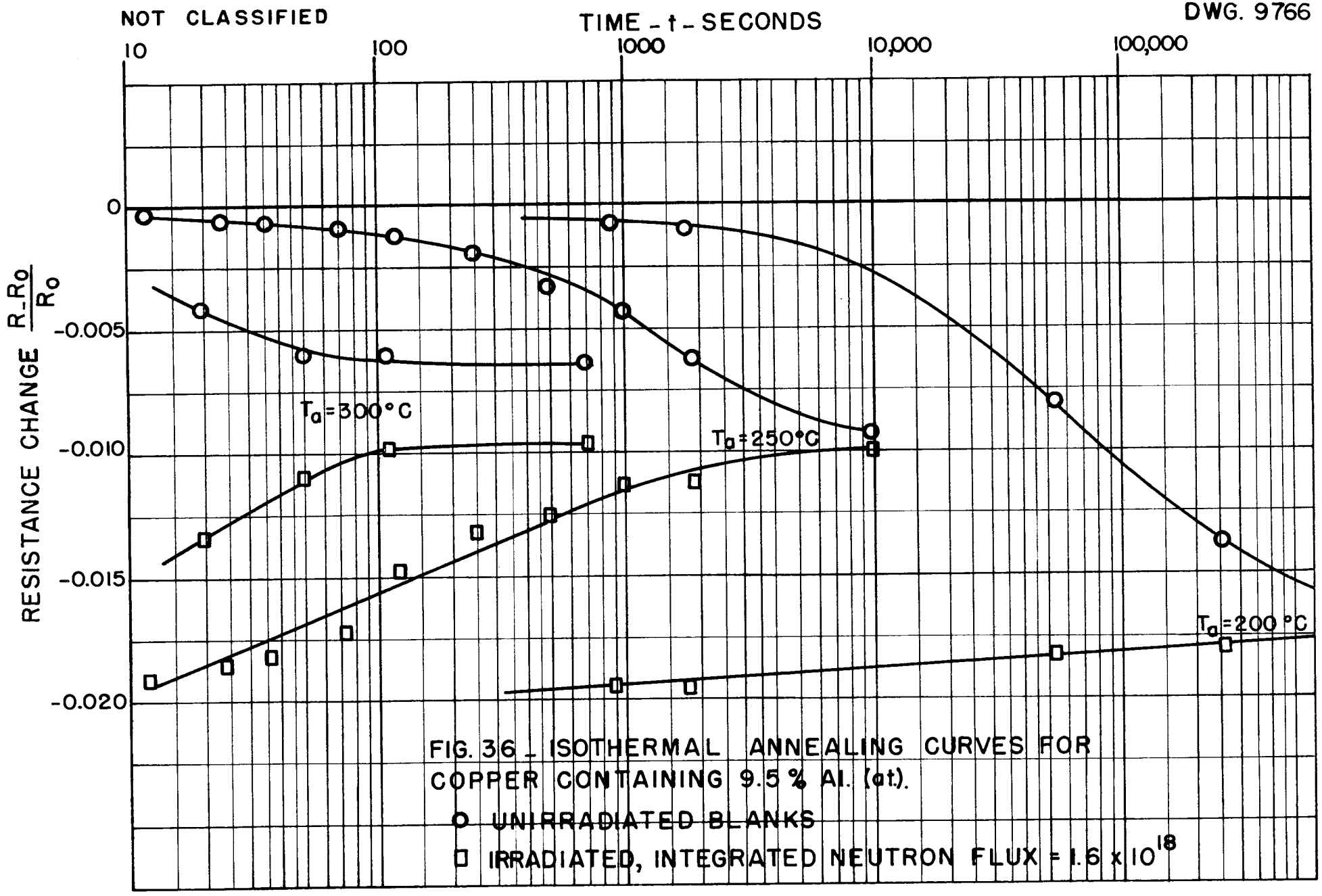

FIG. 36 _ ISOTHERMAL ANNEALING CURVES FOR COPPER CONTAINING 9.5 % Al. (at.).

O UNIRRADIATED BLANKS

□ IRRADIATED, INTEGRATED NEUTRON FLUX = 1.6×10^{18}

The isothermal annealing curves exhibit a number of important characteristics:

1. The irradiated specimens partially recovered their original resistance; the extent of recovery was dependent on the temperature.
2. The unirradiated blank specimens decreased in resistance; the extent of the change was dependent on the annealing temperature.
3. The irradiated specimens and unirradiated blanks approached the same condition of equilibrium as measured by electrical resistance from opposite directions.
4. The shape of the annealing curves for the unirradiated blanks suggests a nucleation and growth process.
5. The shape of the annealing curves for the irradiated samples indicates the absence of a nucleation stage.

Upon completion of annealing, two samples—one irradiated and the other not—were quenched from 700°C. This treatment caused them to return to their original and unirradiated conditions.

The response to annealing of the unirradiated blanks is typical for nucleation and precipitation from a supersaturated solution. The behavior of the irradiated samples can be explained by precipitation from a supersaturated solution during irradiation, followed by re-solution of the precipitate during annealing. If this is true it is the first instance to be reported of a precipitation reaction activated by irradiation.

Further experiments are planned to verify this hypothesis, to determine the effect of irradiation on reaction rate, and to determine what impurity is taking part in the reaction.

X-ray investigation of Cu-Al alloys showed no significant difference in the lattice parameters before and after irradiation. A very slight broadening and apparent weakening of the lines in the back-reflection region was observed after irradiation of 1% aluminum sample. No change was observed for the 9.5% aluminum sample.

Photomicrographs were made of specimens of the Cu-Al alloys containing 0.26% and 4.28% Al by weight, Cu-Si alloy containing 2.5% Si by weight, Cu-Be alloy containing 2% Be by weight, and pure Cu, before and after irradiation. The microstructures were not altered by irradiation.

IN-PILE CREEP EXPERIMENT

Several models of the in-pile creep apparatus described in ORNL 576[3] have been constructed and bench tested. The apparatus utilized 1/8 in. diameter specimens (304 stainless in first test) with a four-inch gage length, operated at 1200°F. Loading is supplied by dead weights outside the pile; a microformer connected to extensometer elements welded to the ends of the gage length, measures the extensions. The special stringers and hole plug to allow insertion of this device in a side hole in the ORNL reactor are being fabricated. The apparatus should go into the reactor not later than the third week in August.

The main improvements have been in small features of mechanical design and the temperature control system. A combination of a Leeds and Northrup Speedomax recorder and DAT control unit working from a thermocouple on the test bar has decreased the periodic temperature variation on the test bar to less than ± ½°F. Certain aperiodic variations of about two degrees are being studied to determine their source.

In operation the apparatus will be inserted into the reactor during one of the scheduled shutdown periods and loaded immediately so that a creep curve over perhaps a six-hour period will be available before the reactor is started. In this way it is hoped to get into the region of so called "secondary stage" creep before irradiation so that if there is an effect of neutron bombardment it may be more readily seen. If no effect is shown here, the creep rate for about six days will be observed prior to the next shutdown, and the variation of rate, if any, closely followed in the absence of the flux during this shutdown.

(3) Brundage, W. E. and Primak, W., "Irradiation Creep Experiment," *Physics Division Quarterly Progress Report for Period Ending December 15, 1949*, ORNL 576, 8 (Feb. 7, 1950).

SERVICE WORK

MELTING, DRAWING AND EXTRUSION

Fuel Rods for CP-3 Reactor. The fabrication of fuel rods for the CP-3 heavy water reactor at Argonne National Laboratory has been concluded. This work required a total of 83 ingots of aluminum-enriched uranium alloy containing 2% uranium. The alloys were prepared by melting, in a high frequency induction furnace, 99.9% pure aluminum and adding enriched uranium metal to the molten aluminum. The metal was cast into a 3-1/16-in. diameter graphite mold. The finished ingots were cut into two extrusion billets. The billets were extruded and the extruded rod was rolled to the required size of 0.850-in. diameter. This work has been described in detail in a separate report.[1]

Enriched Uranium-Aluminum Slugs for Hanford. The Metallurgy Division of Oak Ridge National Laboratory was requested to make 10 enriched uranium-aluminum slugs by casting billets, then extruding these billets to produce rods from which the slugs were machined. Two ingots of 7½% enriched uranium and 92½% aluminum were cast in 4-1/16-in. diameter molds. These ingots were then extruded through a 1½ in. flat face die. The 10 enriched uranium-aluminum slugs were machined from the extruded rods. This work has been reported in a memorandum to Dr. R. J. Ward at Hanford.[2]

ROLLING MILL

Sheathing of Enriched Uranium-Aluminum Slugs for Exposure to the Chalk River Reactor. The Metallurgy Division was requested to fabricate a Chalk River fuel assembly using 10 enriched uranium-aluminum (7½% uranium) alloy slugs plus the necessary spacers of 2S aluminum. These slugs were furnished by Hanford; the sheath and closure plugs were sent from Chalk River to the Oak Ridge National Laboratory. The 10 enriched uranium-aluminum slugs and the 2S aluminum spacers were drawn in the Chalk River sheath using a 20,000 lb Standard Machine Drawbench. After drawing the assembly, the end plugs were brazed onto the outside of the sheath. This sheathing operation was the subject of an ORNL memorandum.[3]

(1) Manly, W. D., *Extrusion of 2% U-Al Alloy Fuel Rods for the Argonne CP-3 Reactor*, ORNL 766 (July 26, 1950).

(2) Manly, W. D. to Ward, R. J., *A Letter Regarding Fabrication of Ten Uranium-Aluminum Slugs*, ORNL CF 50-6-113 (June 16, 1950).

(3) Erwin, J. H. and Manly, W. D., *Sheathing of Enriched Uranium-Aluminum Slugs for Exposure in the Chalk River Reactor*, ORNL CF 50-6-147 (June 26, 1950).

Ferroboron for Adjustable Neutron Slit. A request was received from the Physics Division for ingots of boron steel containing 7% boron to be fabricated into an adjustable neutron slit. Two ingots measuring 1¼ in. × 4¾ in. × 8¼ in. were prepared by melting in a high frequency induction furnace and casting into a graphite mold. The alloy was dense and hard, having a Rockwell hardness of 67 on the *C* scale. This extremely hard material was also quite brittle and difficult to machine to the required shape. It was then suggested that the piece be fabricated by powder metallurgy and test pieces of carbonyl iron with 7% natural amorphous boron were prepared at NEPA by pressing the powdered metals at 1000 psi and 850°C and 1030°C. The material sintered at the lower temperature showed a considerable variation in hardness from the center portion (R_B84) to the outer surface (R_B60). The density of this piece when sampled at different points varied from 4.6 g/cc to 5.4 g/cc. This represents a variation of 70% to 80% of theoretical density (6.73 g/cc), and as might be expected, the microstructure showed a porous structure with numerous voids. The sample pressed and sintered at 1030°C still showed a slight variation in hardness ranging from R_c50 at the surface to R_c60 at the center. However, the measured density was very uniform at 6.63 g/cc (98.5% theoretical density).

The increase of hardness produced by the higher sintering temperature again presented fabrication difficulties, therefore it was decided to press the final piece containing B^{10} at 850°C and 1000 psi. This work is now being done at the Materials Laboratory of the NEPA project.

Other Service Work. Further service work performed for various divisions at ORNL and groups within the Metallurgy Division includes the following:

1. Preparation of five pounds of cast thorium in the form of ¼ in. × ¼-in. bars for NEPA.
2. Casting of four sheet ingots of natural uranium.
3. Preparation of samples of silver and silver alloys (Ag-Cd and Ag-In) for internal friction studies.
4. Casting of sheet ingots of Al and Al alloys for rolling experiments for the Reactor Technology School. The alloys considered for three ingots each of 2½% Mg - 97½% Al and 2% U - 98% Al.
5. Casting 4-1/16-in. diameter ingots of copper and brass for extrusion billets to be used in preferred orientation studies.

6. Preparation of Cu-Ge and Cu-Ga for radiation damage studies.

7. Preparation of Pb-U and Pb-Bi alloys for ANP program.

8. Preparation of alloys of Fe-Co and Fe-Si for Physics Division to be used in preparation of single crystals.

9. Remelted gold for rolling into gold sheet for Materials Laboratory at Y-12 area.

10. Extrusion of zirconium and zirconium alloys for Westinghouse.

PERSONNEL

J. H. Frye, Jr. - Director

E. J. Boyle - Assistant Director

L. E. Banker - Administrative Assistant

L. K. Jetter - Technical Advisor to the Director

Roberta Hudson, Secretary

Helen Carr, Secretary
Doris Jacox, Stenographer
Dolores Poe, Stenographer
Jane Thomas, Stenographer
Katy Childress, Stenographer

A. G. H. Andersen	Mechanical Testing, Properties of Pure Metals, Creep of Uranium, and Stress Rupture Testing	C. W. Weaver J. W. Woods R. T. Clem
D. S. Billington	Fundamental Radiation and Physical Metallurgy and Radiation Damage	F. M. Blacksher
T. H. Blewitt	Fund. Rad. and Physical Met.	
G. T. Murray	Fund. Rad. and Physical Met.	
W. E. Taylor	Fund. Rad. and Physical Met.	
M. J. Feldman	Radiation Damage	
J. T. Howe*	Radiation Damage	
J. C. Wilson	Radiation Damage	
J. C. Zukas	Radiation Damage	
B. S. Borie, Jr.	X-ray Diffraction	
R. J. Gray R. S. Crouse	Metallography	E. R. Boyd E. P. Griggs B. C. Leslie
L. K. Jetter	Fundamental Physico-Metallurgical Research	J. C. Ogle
G. H. Boss		
C. D. Smith	MTR Development and Rolling Mill Activities (charge of 101-B Bldg.)	G. E. Cooley C. F. Cutcher J. B. Flynn J. N. Hix H. J. Wallace

* Dual Capacity

[redacted]

PERSONNEL (cont'd)

L. G. Glasgow		
W. D. Manly	Thorium Research and Alloy Development, Physical Metallurgy of Al-U Alloys, Casting, Mechanical Working, and Heat Treating	
J. H. Erwin	Physical Metallurgy of Al-U Alloys (charge of Metal Working and Heat Treating Room in 101-D)	G. D. Goldston D. E. Rosson J. P. Turner
D. E. Hamby	Thorium Research and Alloy Development (charge of Melting and Casting Room)	D. O. Buker E. E. Layne C. J. Zachary
R. O. Williams	Thorium Research and Alloy Development, Physical Metallurgy of Al-U Alloys	D. S. Easton
E. C. Miller	ANP Materials	T. W. Fulton R. W. Johnson J. E. Pope C. L. Smith L. R. Trotter R. M. Wallace R. S. Webb
L. A. Abrams		
G. M. Adamson		
E. S. Bomar, Jr.		
W. H. Bridges		
J. E. Cunningham		
R. B. Day		
F. W. Drosten		
J. T. Howe*		
R. B. Oliver		
P. Patriarca		

ACTIVE CONSULTANTS

E. Creutz	ANP
N. J. Grant	ANP
J. L. Gregg	ANP and Metallurgical Coordinator of Beryllium for the MTR
E. E. Stansbury	General Consultation
D. K. Stevens	ANP

*Dual Capacity

[redacted]